ZECHSTEIN SALT DENMARK
Salt Research Project EFP-81

Volume III
Fabric analysis of domal rock salt

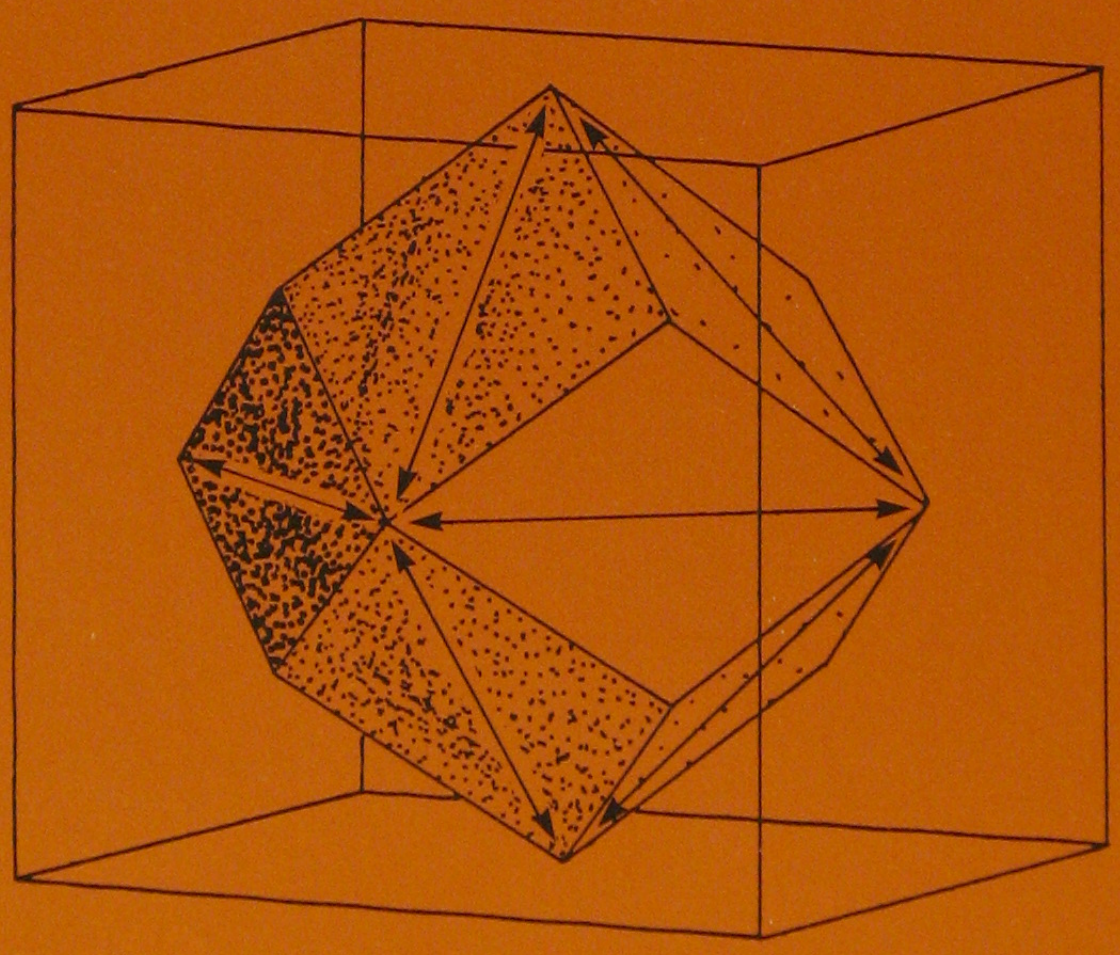

DGU
Geological Survey of Denmark
1984

VOLUME III

E R R A T A .

Page 14. Line no. 11 and 16: "comprices of" read "consists of"

- 15. - 19: "comprise of" read "consist of"

- 18. - 2 from below: "(<30)" read "(<30°)"

- 20.Fig. 4 a-e. Line no. 6: "perpendicular" read "parallel"

- 11: Delete "Note, that ...."

- 21. Line no. 1: "foldaxes" read "fold axes"

- 27. - 25: "table 2" read "table 1"

- 31. - 8: "line covariance" read "line and covariance"

- 35. - 14: "EFF-factors" read "EFF-values"

- 40. - 3: "cm" read "cm^2"

- 37: "Figure 14" read "Figure 15"

- 43. - 20: "fig. 15" read "figure 16"

- 50. - 4: "figures A-D" read "figures A, C & D"

- 52. - 15: "(1982)" read "(1983)"

- 55. - 4: "axes), 2)" read "axes) or 2)"

- 56. - 29: After "study" add ", which is based on the short-term uniaxial compression tests performed at room temperature,"

- 57. - 25: "caverns" read "vertical cavern walls"

- 1 from below: "technic" read "technique"

- 60. - 4: "(pattern 1) one" read "(pattern 1) is one"

- 5: "another" read "another one"

- 19: "relative" read "relevant"

- 22: After "that the" add "short-term uniaxial and vertical"

- 61. - 21: "idenpendent" read "independent"

- 33: "agreement" read "argument"

Page 39, Fig.14; page 43, Fig. 16; page 44, Fig. 17 a & b: "table I" read "table II"

ZECHSTEIN SALT DENMARK
Salt Research Project EFP-81

Volume III
Fabric analysis of domal rock salt

By Jørgen Gutzon Larsen
Per Lagoni

July 1984

DGU-[redacted]series C no. 1 · 1984

ISBN 87 88640 08 6 (bd. 1-4)

DGU
Geological Survey of Denmark

PREFACE

Volume III is part of four volumes elaborated in the course of Salt Research Project EFP-81.

The volume deals with petrofabric analyses of rock salt related to mechanical test data and statistical analysis of these data.

CONTENTS

CHAPTER 1.

TEXTURAL AND PETROFABRIC ANALYSES OF ROCK SALT RELATED TO MECHANICAL TEST DATA - A QUANTITATIVE APPROACH

By Jørgen Gutzon Larsen

CONTENTS

TEXTURAL AND PETROFABRIC ANALYSES OF ROCK SALT RELATED TO MECHANICAL TEST DATA - A QUANTITATIVE APPROACH.

ABSTRACT

Textural studies have been performed on rock salt cores from the Tostrup and Mors salt domes as part of a general structural study with the purpose of quantifying textural descriptions and relating them to uniaxial compression strength of the rock salt.

The textural analyses are performed on replicas of cut and grinded rock salt surfaces, which have been stored in oversaturated NaCl solution so that the crystals have started to grow. By this treatment each crystal is easy to identify and draw up. Copies of the replicas are used for automatic image analyses where maximum crystal length, area and perimeter are measured for each crystal. These data are used to calculate average crystal size, specific perimeter (perimeter/area) and an ellipsis form factor EFF. The latter compares the measured perimeter with that of an ellipsis in order to quantify the surface ruggness as a measure for the intergrowth and coherence of the sample.

The analytical results show the presence of different types of grain size distribution apparently unrelated to the stratigraphy or degree of deformation. The deformation axes of the halite crystals show that the Tostrup salt is deformed in a complex triaxial stress field. The degree of deformation of the rock salt is estimated to range from 5-75 %.

Petrofabric measurements have been performed on regrown spherical samples up to 10 cm in diameter mounted on a special universal stage. The stage is moved stepwise under a beam of parallel light and reflections are noted. The fabric pattern shows that the Tostrup rock salt is anisotropic with (100) pole maxima subparallel to the strain axes a, b and c and with a girdle of (100) poles situated within the foliation plane. Maxima may also be

diagonal or oblique oriented relative to the deformation axes. There are several possible explanations for the fabric patterns, of which 1) syntectonic recrystallisation or 2) intragranular translation gliding along slip systems of the halite seems most likely. The oblique maxima may be due to overprinted fabric patterns perhaps caused by recent differential movements.

The textural study has shown, that uniaxial compression strength of rock salt is dependent on grain size, dip of foliation and degree of flattening, a/c. Fine grained rock salt is generally stronger than the more coarse types. Increasing dip of foliation correlates with decreasing compression strength along different correlation lines. Higher compression strength of the steeply foliated rock salt is shown to correlate with lower a/c ratios and lower ellipsis form factor, EFF, typical of the Zechstein 2 rock salt of Tostrup-8,-9 & 10. Conversely the steeply dipping Zechstein 1 rock salt of Tostrup-6 with high a/c ratios and high ellipsis form factors has low compressive strength.

I. INTRODUCTION

1. The scope of the study

The Tostrup salt dome, situated in northern Jutland (fig. 1) in the Danish-Norwegian Basin, has been selected by Dansk Olie & Naturgas A/S (D.O.N.G.) for storage of natural gas, and 8 wells have been drilled in the search for pure rock salt suitable for cavern leaching. There are two essential questions related to this project: a) what type of rock salt is best suited for construction of caverns? and b) where is this salt located and how is it detected most economically?, i.e. with the least amount of drilling.

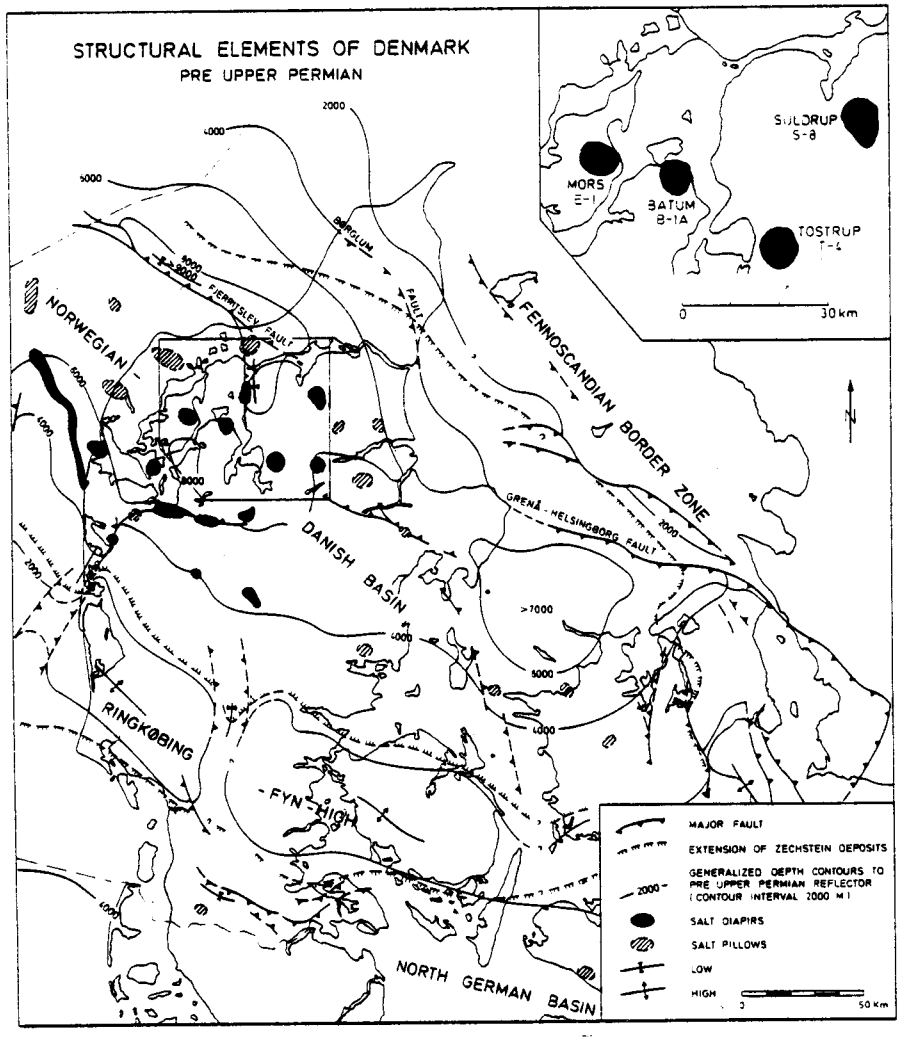

Fig. 1. Map of the halokinesis area, Jutland, Denmark.

a) The evaluation of the stability of the projected caverns is based on mechanical tests on rock salt cores

withdrawn from the cavern depth. The mechanical tests have involved short term uniaxial and triaxial tests together with "long term" creep tests. The results of the uniaxial compression tests showed a large variation of 12-35 MPa, which indicates that during short term pressure drops to atmospheric pressure in the caverns the rock salt may behave differently. In addition closure rates due to creep is expected to differ. In contrast triaxial mechanical tests suggest that the mechanical properties of the rock salt is rather homogeneous under a certain amount of confining pressure. Ottosen & Krenk (1982) have given a review of the mechanics of caverns in rock salt together with mathematic models.

b) In the exploration for pure rock salt it is important to determine the stratigraphy and structure of the rock salt in the wells and to extrapolate the structure as far away as possible from the wells. The complicated folding structure of the domal rock salt makes this rather difficult and all information concerning orientation of the stratification, texture, colour and trace mineral content may be valuable tools in revealing the folding structure.

The scope of the present work has been to develop methods for systematic textural analyses including petrofabric measurements, partly as a general petrographic description in which crystal shape and crystallographic orientation are related to the major structures and deformation history, and partly whith the purpose of relating quantified textural parameters to rock mechanical test data.

The study has been limited to the uniaxial compression tests in order to explain the large variation in the obtained strength values. The data from textural analyses have been handed over to a firm of consulting engineers, LIC-consult, where they have been used in a statistical analysis of the mechanical properties of rock salt (LIC-consult, chapter 2.).

The present work should be regarded as examples of methods and parameters, which may be usefull in the textural description of rock salt. A preliminary report has been given by Larsen (in press).

2. Geological background.

The rock salt of the Tostrup salt dome and other salt domes in the Danish Trough is of Upper Permian age, where four main evaporite cycles, Zechstein 1, 2, 3 and 4 were deposited in the German and the Danish-Norwegian Basins. The stratigraphy of these deposits are described in Vol. II. Zechstein 1 comprises of black shale, dolomites and anhydrite overlain by ca. 400 metres grey rock salt and on top a thin layer of anhydrite formed as a residual of dissolved rock salt before the beginning of the next evaporite cycle.

Zechstein 2 again comprices of a ca. 15 metres thick sequence of black shale, limestone, dolomites and anhydrite followed by ca. 400 metres of grey rock salt resembling the Zechstein 1 grey salt. On the top of this follows a section of reddish-brown rock salt and a potassium-magnesium zone (Veggerby) 50-75 metres in total.

Zechstein 3 begins with 15-60 metres of salt clay followed by ca. 100 metres rock salt with varying reddish and yellowish colours. In the salt are found one layer of potassic salt and one primary and several secondary layers of anhydrite.

Zechstein 4 consists of up to 60 metres of a mixture of clay/silt and coloured rock salt.

These sequences of horizontally sedimented evaporites were mobilized in Late Triassic times by the temperature and pressure increase caused by the deposition of triassic sediments, the pillow stage, (Vol. II and IV). The structural development of salt domes has been

described by Trusheim (1957). The main diapiric penetration phase commenced in Late Jurassic times (e.g. Richter-Bernburg, 1981; Petersen, 1983) and the original horizontal stratification became strongly distorted in a complicated fold structure. The search for pure rock salt of Zechstein 1 or 2, which is expedient for cavern leaching is impeded by this complicated structure, (Jacobsen, 1982).

In the case of cavern leaching it is highly important to know the strength of the rock salt in the cavern area and the suitability for leaching of this salt. These matters are dependent on the shape of the salt grains, the grain contacts, the steepness of the foliation, the content of anhydrite etc. The extracted cores therefore are carefully examined, described and tested at the well site and in the laboratories.

II GENERAL DESCRIPTION

1. Core material.

The rock salt samples from the Tostrup salt dome comprise of 9 m x 100 mm drilled cores, generally with one core taken under the salt mirror and a core every 50 m in the cavern depth,- half of those are oriented.

The entire core can only be examined at the well site, where the geological description and photographic documentation is completed. After this it is divided into samples for the mechanical tests, chemical analyses and type pieces for the Geological Survey of Denmark (DGU).

2. Petrography

a. The anhydritic rock salt banding: The rock salt of the Tostrup salt dome is a nearly mono-mineralic rock

containing bands of anhydritic rock salt, but otherwise is composed essentially of halite, which show a large range in grain size and textures (the potassium-magnesium salts are not delt with in this report). The anhydritic banding in the rock salt represents the original horizontally precipitated bed. The banding is formed by a few per cent of tiny box-shaped anhydrite crystals as aggregates or disseminated in the rock salt. The banding ranges in thickness from a few cm to several meters. Stratigraphic upwards may be indicated by upwards gradation, but examples of the reverse have been reported in Germany (Richter-Bernburg, 1968). Half rosettes

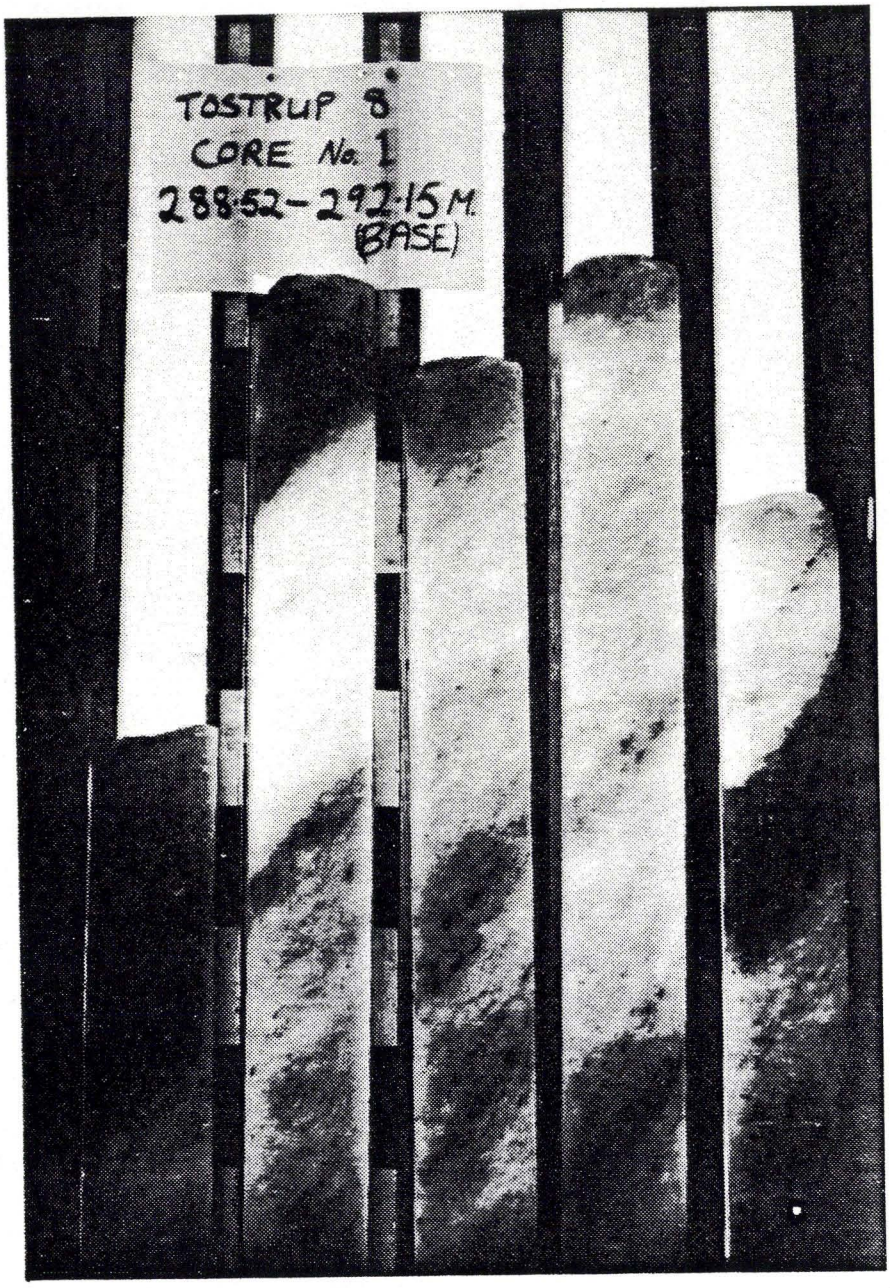

Fig. 2. Anhydritic bands in pure rock salt. Transmitted light.

representing upwards growing tiny anhydrite crystals may occur as thin bands in the larger relic halite crystals (Jacobsen pers. com.). An example of both small scale and large scale anhydrite banding is shown in fig. 2. Lumps of laminated, contorted anhydrite several cm in size may occur, especially close to the dolomite-anhydrite zone between Zechstein 1 and 2 (Jacobsen, pers. com.). The orientation on the anhydrite banding is measured as a routine work and it is used for establishing the folding structure.

b. Classification of the rock salt: The rock salt is classified into fine grained (< 1 mm,) seldom present, medium grained (1-5 mm), coarse grained (>5mm) and pegmatitic (>50 mm).

The grain-size may show a restricted range producing a homeoblastic texture, or may show a large variation giving a heteroblastic texture, which in the presence of scattered distinctly larger crystals gives a porphyroblastic texture. The postfix -blastic is generally valid because strong deformation is apparent from the textural examination. In general the crystals do not show any crystal surfaces, i.e. the rock is xenoblastic. The texture may be characterized by a preferred crystal orientation, a gneissic texture, with a more or less pronounced foliation and lineation. The crystal shape of this type of rock salt can be described as more or less irregular flattened ellipsoids or elongated lentils. Rock salt with equant grains and curved surfaces has a granoblastic texture while rock salt with interlobing grain boundaries has an amoeboidal texture. Rock salt of these two types are frequently found in the uppermost cores below the salt mirror. The texture is believed to represent recrystallized rock salt (Richter-Bernburg, 1968, p. 925-926). In some cases primary crystal surfaces have been preserved giving the rock salt a hypidiomorphic texture. Such primary textures have only been recorded in the Z3 salt in the Tostrup wells. Representative textures are shown in fig. 3.

c. Relation between anhydrite banding, foliation plane and strain axes: In general the structural analyses of the cores at the well site are rather brief dependent on the well site geologist: the orientation of the banding is measured, whereas less attention has been payed to the foliation and lineation formed by the deformation of the

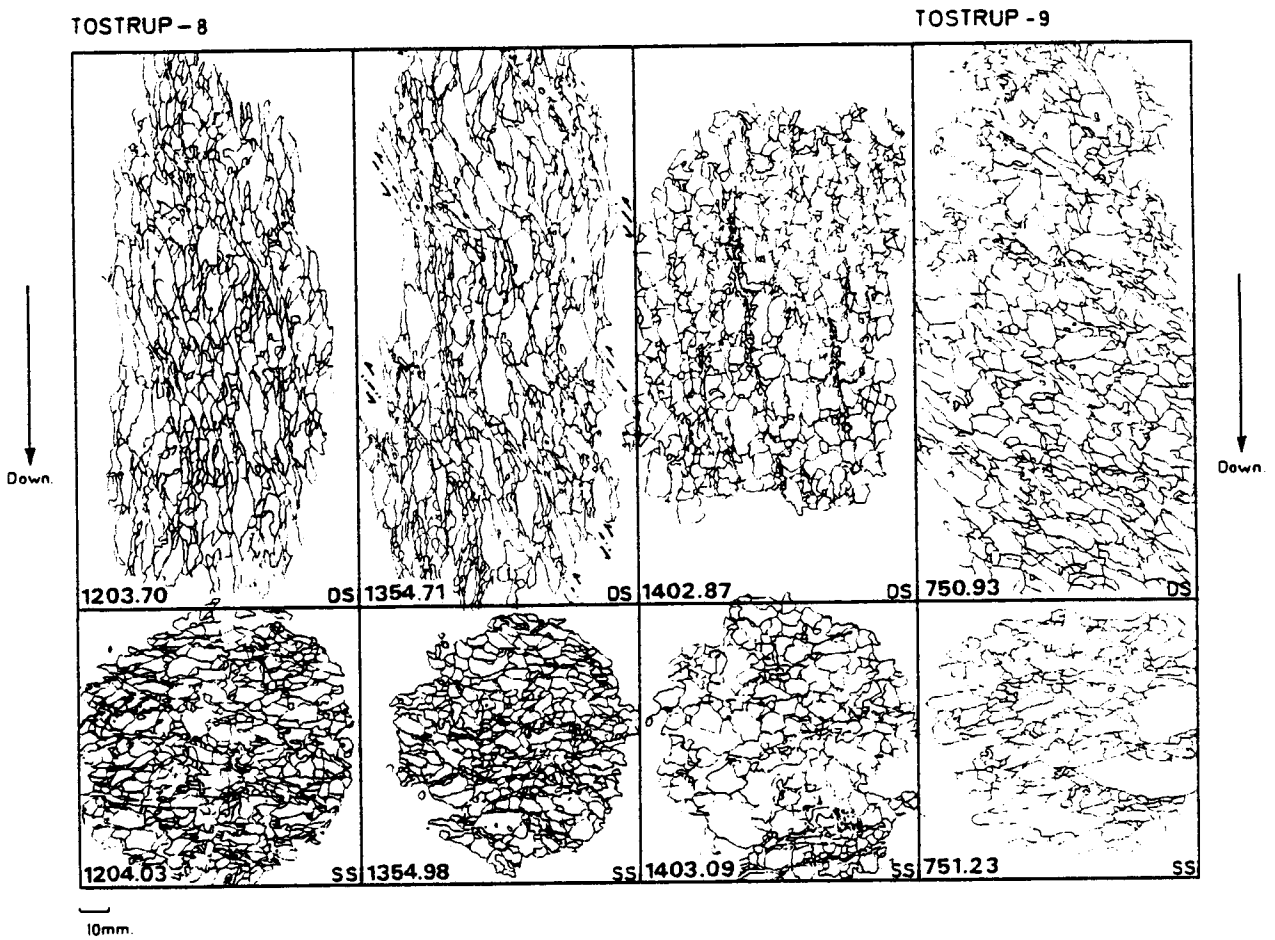

Fig. 3. Representative rock salt textures.

halite crystals. The foliation has a rather constant orientation within each core, but discordant shear zones may occur at the interface between the anhydritic rock salt bands and the pure rock salt. It is believed to be due to a higher competance of the anhydritic rock salt even though the anhydrite content is only a few per cent. In some cases a crystal lineation can be defined on the broken surfaces following the foliation plane. The well site description and laboratory work have shown, that when the lineation is distinct, it tend to be parallel or subparallel (<30) to the dip of foliation. Distinct oblique lineations occur, however. In the present study

the lineation was observed on the cleaved core ends, as cutting parallel to the foliation plane was restricted in order to save core material. In general the cutting of the cores was perpendicular to the strike and to the dip. By this procedure the cut surfaces may not contain the maximum and minimum values of the strain axes. On the other hand the grain shape in the direction of the foliation dip was obtained and this is believed to be important when the textural data are compared to the compression strength. Despite the uncertainty whether the true strain axes are parallel or subparallel to the cut sections the study has shown that in general the a axis (long axis) is mostly subparallel to the dip of the foliation, the b axis (middle axis) is subparallel to the strike of the foliation and the c axis (short axis) is perpendicular to the foliation plane. The terminology is in accordance with that of Sander (1930) but is here used in a purely descriptive way. In some cases the b axis is parallel to the dip direction of the foliation, especially in To-7 (table I in appendix). Friederich (1957) stated, that in small scale folds of the

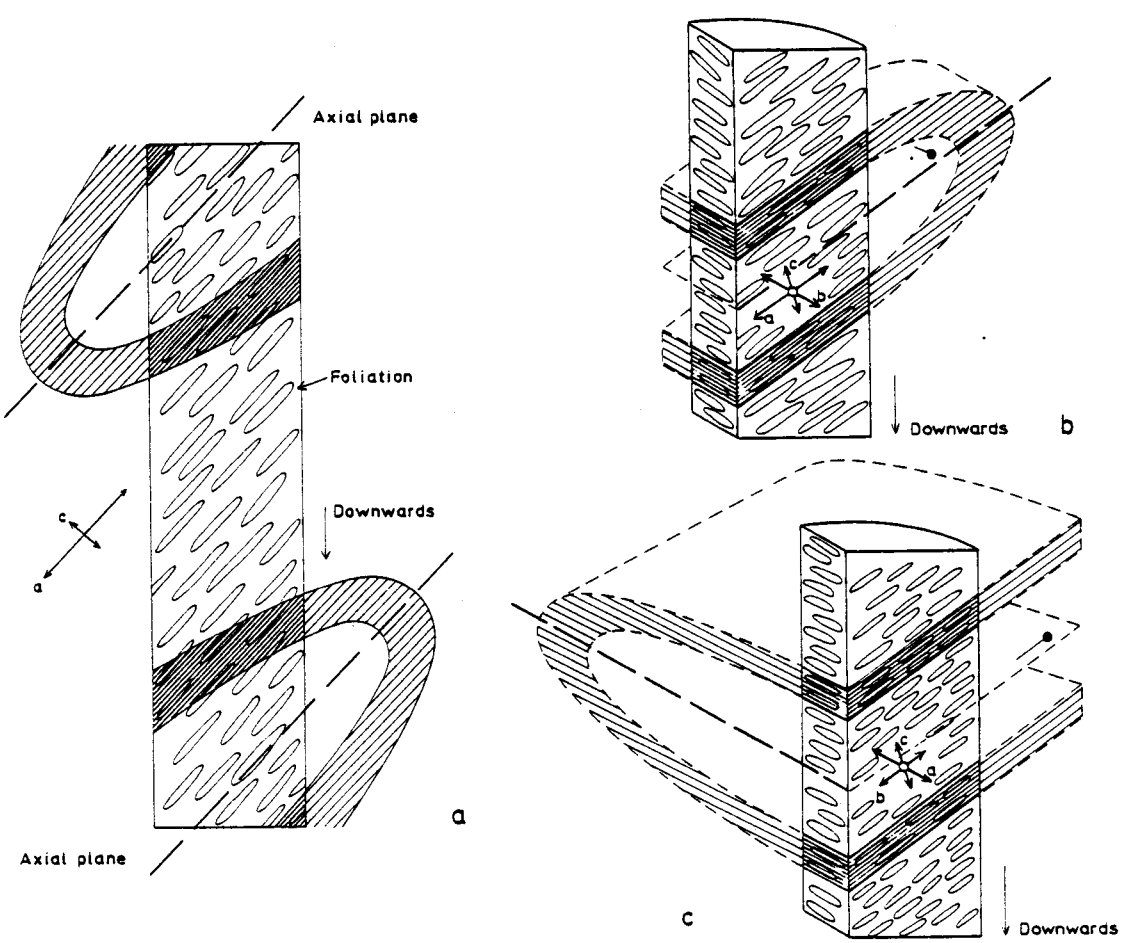

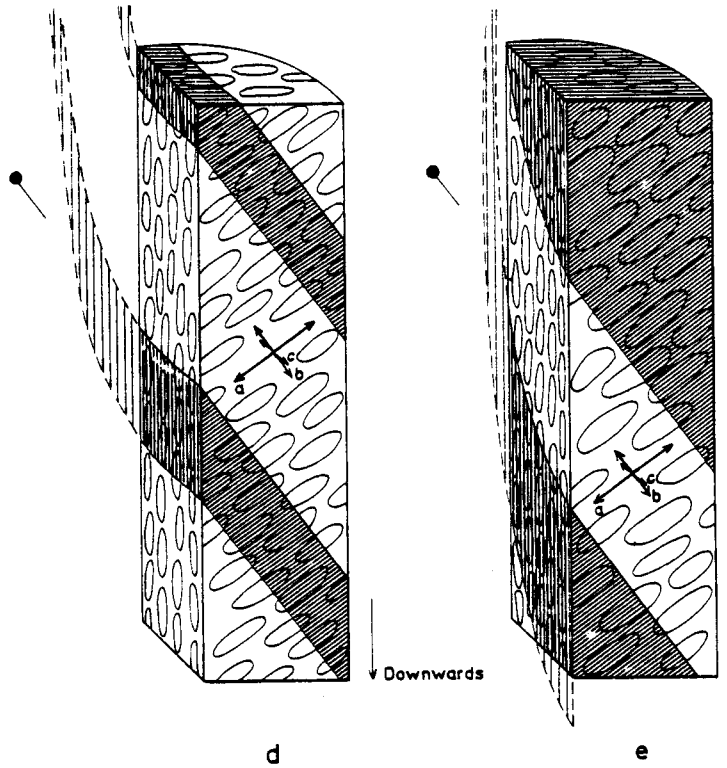

Fig. 4 a-e.

Simple structural and textural relationships in drill core samples showing the relationship between axial plane foliation, strain/fabric axes, and bedding plane of anhydritic rock salt. The interpretations assume that

1) the b axis is perpendicular to the fold axis,
2) the foliation is an axial plane foliation,
3) the a axis is perpendicular to the fold axis,
4) the c axis is perpendicular to the foliation plane.

The size of the fold is strongly reduced relative to the core dimensions. Note, that the a axis could also be parallel to the fold axis.

"Hartsalz" of the Werra area the a axis of the halite is perpendicular to the fold axis, the b axis is parallel to the fold axis and the c axis perpendicular to the axial plane. Clarke & Schwerdtner (1966) found the same relationships in the slightly folded, bedded rock salt of Saskatchewan. It is uncertain whether such simple relationships are valid for the Tostrup salt dome. Here the general orientation of the strain axes in To-6, -8, -9, & -10 would imply a dominance of horizontal foldaxes.

The foldaxes constructed from the anhydritic banding are generally dipping more than 30° for each of the wells and mostly about 50° for all the wells (Jacobsen, 1982). Low dipping fold axes of 0-30° can, however, be constructed for To-5, -6, -8, -9 & -10 for levels down to 1200 m depth using the data compiled by Jacobsen (1982). These wells are situated close to each other. Jacobsen (1982) also noted the low dipping axes in the upper part of the salt dome. He pointed out that these horizontal fold axes may be due to drag folding. Based on the findings of Friedrich (1957) and Clarke & Schwerdtner (1966) some simple relationships between the anhydrite banding and foliation are shown (fig. 4a-e).

d. Microscopic observations: Ordinary thin sections are of little value for the description of pure rock salt, due to its coarse grained nature. At the beginning of the project, however, ca. 3-5 mm thick thin sections prepared in alcohol were used for petrofabric studies, and these "thin" sections were well suited for examinations under the stereomicroscope:

The halite crystals contain scattered tiny box-shaped anhydrite crystals obviously with a random orientation. They seldom cross the grain boundary. In addition, most crystals have cube shaped gas-liquid inclusions which are situated dominantly along the cubic cleavage planes and less frequently along somewhat irregular planes corresponding to the glide planes (110). It was not possible to relate the liquid inclusions to an original crystal surface as the planes of liquid inclusions cut each other. Therefore the inclusions have formed along annealed cleavages (see Fabricius, in press (Vol. IV)) under which conditions the liquid inclusions formed). Often the (100) cleavages or healed cleavages are rotated showing extensive deformation of the crystals. Thin sections of the short term uniaxially tested samples show an increased number of (100) cleavages, often strongly deformed, together with strongly curved, irrregular cleavages which might correspond to the (110) glide planes. In addition, break up of the grain boundaries is

typical for the vertically foliated Tostrup rocks salt. In the untested rock salt air bubbles are present on the boundaries of the crystals, but these have presumably formed during the preparation of the thin section. In many rock salt cores there is a considerable capillary force, which is observed when the surface is covered with an organic liquid based colour. This is belived to be due to loosening of the grain boundaries caused by the vibrations of the drilling and the physical changes imposed during the withdrawal and later handling of the core, Fabricius (1980). Rock salt with a low coherence, e.g. To-6 salt, is naturally mostly affected by these processes.

III. TEXTURAL ANALYSES

1. Introduction

Several parameters are of interest in the textural analyses: Measurements of 1) length, 2) width and 3) thickness of the grains, corresponding to the a, b and c-axes of the strain ellipsoid 4) grain area, 5) grain perimeter and 6) degree of alignment.
It is very difficult to obtain the true values of these parameters especially on a cut surface because it represents all kind of sections in irregular ellipsoid or lensoid crystals. Relative differences between the salt cores, however, are equal important as exact values for the present study. For this reason there has been no attempt to make corrections on the measured data in order to obtain the true values. Neither has the degree of alignment of the individual crystals been measured; this parameter is believed to be incorporated into the length/thickness ratio.

2. Sample preparation.

The core samples for the textural work were 50-70 cm long. They were examined for the orientation of the

plane of crystal foliation (cleavage plane) and the lineation. In order to obtain textural data which are directly meaningfull for the compression tests, the samples were cut 1) perpendicular to the strike of the foliation plane, 2) perpendicular to the dip direction and 3) parallel to the foliation plane (only i some cases in order to save core material).

The cutting was performed with a diamond saw using small amounts of water for cooling. The structural analyses have shown, that generally the cut sections are approximately perpendicular to the long axis, middle axis and short axis of the halite crystals, and thus give a picture of grain shape and dimension. For the measurements of these axes, designated the a, b and c axes, only the a-c and b-c sections are needed. The cut and grinded surfaces give a good impression of the texture of the rock but are not suited for the detailed measurements performed in this study by using automatic image analyses, and also the documentation, i.e. the polished surfaces do deteriorate. Several methods were applied in order to make the crystal boundaries distinct, but the success of these was strongly dependent on the presence of open grain boundaries. The most succesfull method is described below:

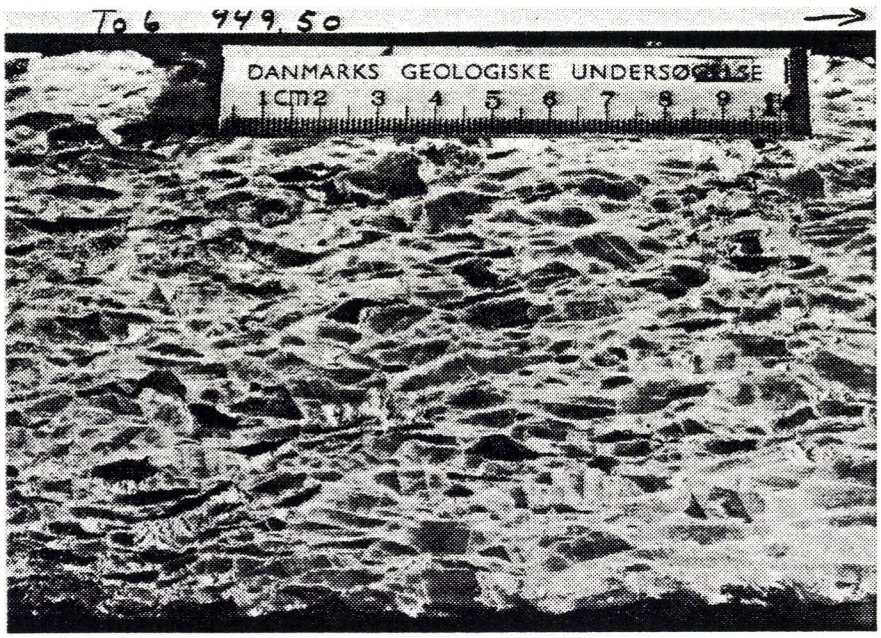

Fig. 5. Photo of a rock salt slab.

The cut rock salt is grinded to form an even surface and

the grinding is completed with a fine grade corundum paper (fig. 5). The surface should not be polished. The sample is placed 2-4 hours in a slightly oversaturated NaCl brine, which is allowed to evaporite

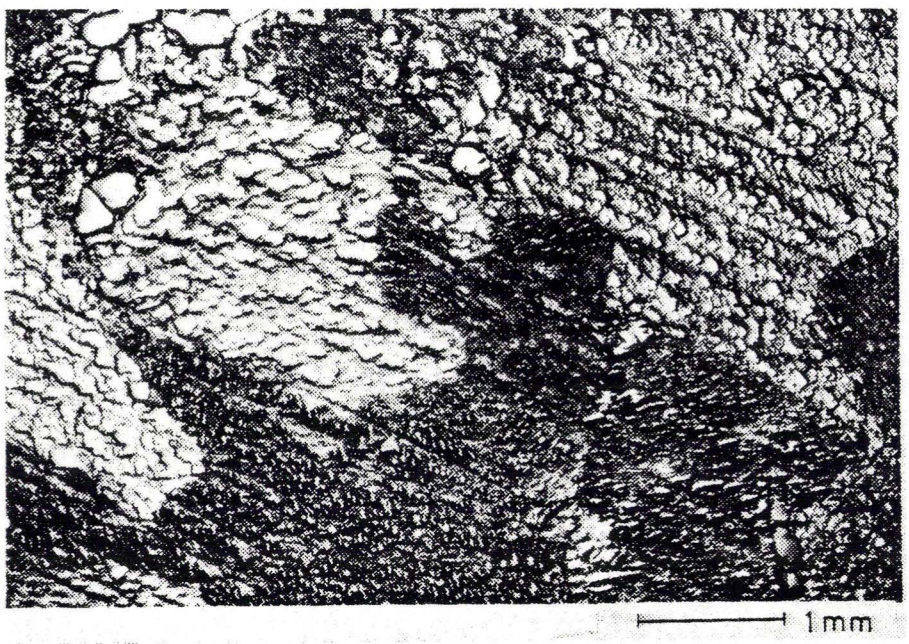

Fig. 6a. Microphoto of a rock salt slab where the crystals are covered by Haüynian cubelets, precipitated from a NaCl solution.

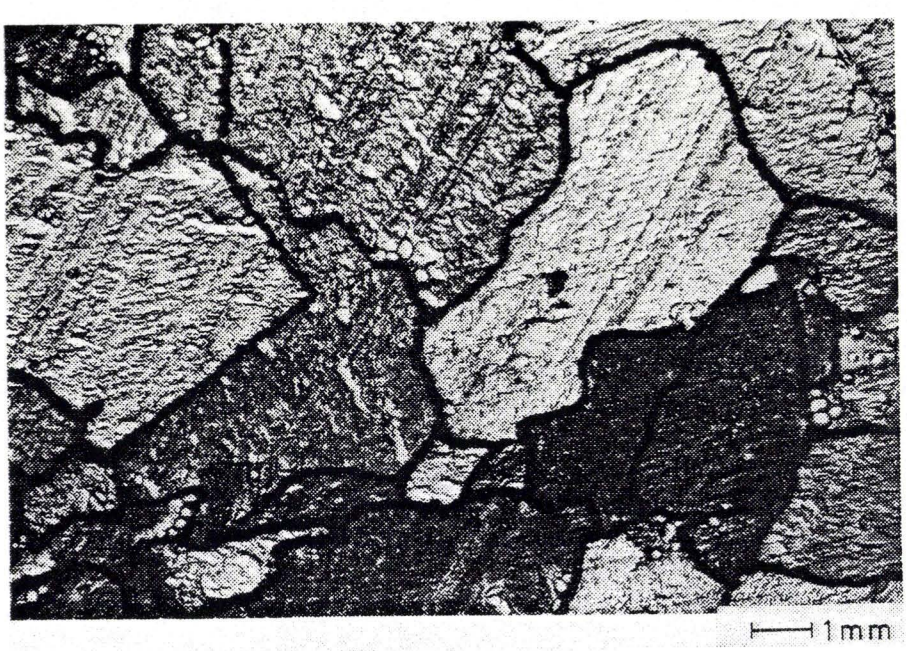

Fig. 6b. Microphoto of a replica with outlined crystal boundaries.

slowly. Each crystal starts to grow, forming Haüynian cubelets along the groove marks from the grinding (fig. 6a). A replica, e.g. an acetate film 0.24 mm thick, is

produced of the surface by covering the latter with acetone and rolling the film over, so that air bubbles and excess acetone are removed. The presence of holes or cracks will spoil the replica. The film is removed after some minutes, dried, and later ironed. It will shrink ca. 10%. Due to the different orientations of the Haüynian cubelets the crystals will show different light intensities, changing with the direction of the light. The replica cannot be used directly to the image analysis because the light contrast between the individual crystals is too small. For this reason, the grain boundaries were drawn up with a tusch pen (0.1 mm) under a steromicroscope (fig. 6b). In this way it was certain, that the image analyser could "see" each grain, although some details have been covered with tusch.

3. Analytical methods

a. Manual methods: 1) The maximum length, projected on the general foliation plane and the maximum thickness projected at right angle to the foliation plane were measured (table II, appendix) and treated statistically in fig. 7. This method gives the best data base for the coupled length-thickness relationship for each grain; however, the area and perimeter of each grain cannot be measured, and the work is time consuming. 2) Grain counting traverse is an easy way of obtaining average values. The amount of grains cut by a line of a given distance is counted. This method is rather quick and can be performed directly on the replica without drawing up the grain boundaries. By this method only average length and thickness can be obtained and neither area nor perimeter can be measured. A few measurements are given in table 1, where they are compared with the automatic image analyses.

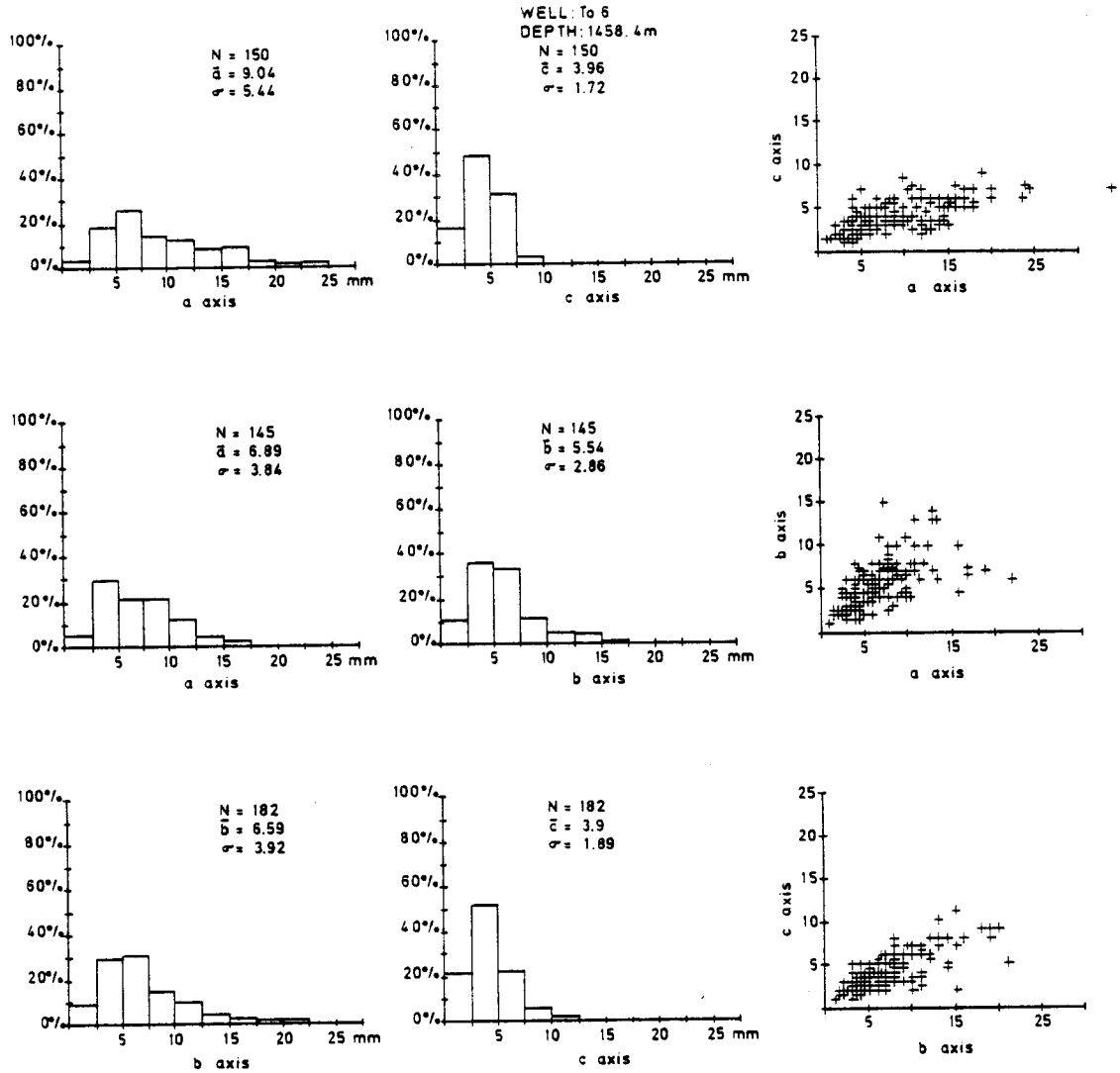

Fig. 7. An example of grain dimensions, size distribution and axial variation according to manual measurements. N= number of measurements. a,b and c are average size. σ = standard deviation.

Table 1. Grain size by manual linear counting and automatic image analyses.

	To-8, 760	To-8, 822	To-10, 898
a m.l.c.	4.89	6.31	4.38
a a.i.a.	4.88	6.20	4.65
c m.l.c.	2.75	3.14	3.15
c^* a.i.a.	2.70	2.91	3.03

m.l.c. : manual linear counting method by a 5 mm grit.
a.i.a. : automatic image analyses.
c^* : short axis calculated from the average grain dimensions.

b. Automated methods: Image analyses were performed on a Leitz TAS at The Technological Institute, Tåstrup. The analyses are superior with respect to measurements of one of the grain dimensions (maximum length or width) area and perimeter, but coupled length-thickness values could not be obtained within the same measurement. The other dimension had to be measured in another run. The perimeter has been measured by subtracting the area inside the grain boundary (tusch boundary) from the same area plus a layer of points around this area formed by automatic dilatation of the grain. The parameters for each grain or average values for a certain area can be measured. Individual grain measurements were selected in order to see how the different parameters are related to the grain size. Due to limited finances, however, only the maximum length of the grains were measured and the average width and ellipsis width were calculated from the length and area of each grain. The analyses were checked against known standards. The ellipsis width, c^*, calculated form the average area (A) and average length (L) is lager than the calculated average width, c. (see table II in appendix) because c^* is weighted with respect to the area. The c^* does agree with average values obtained by the linear counting method as exemplified in table 2 for both the length and the thickness. Actually measured maximum width, should be compared with the maximum length, but as long as the parameters are measured by the same method, they are usefull for the present study even though the grain dimensions are not the true ones.

4. Results of the automatic image analyses.

a. Characterization of the rock salt by area distribution in relation to maximum grain size:
Typical frequency distributions relating the amount of grains and their covered area to crystal size in 2 mm intervals are shown in figs. 8 a-d. (All the analyses are stored at DGU). The amount of grains decreases more

or less asymptotically with size. There is a continuous size range from 0-30 mm in some samples and from 0-70 mm in others, showing that the rocks are generally

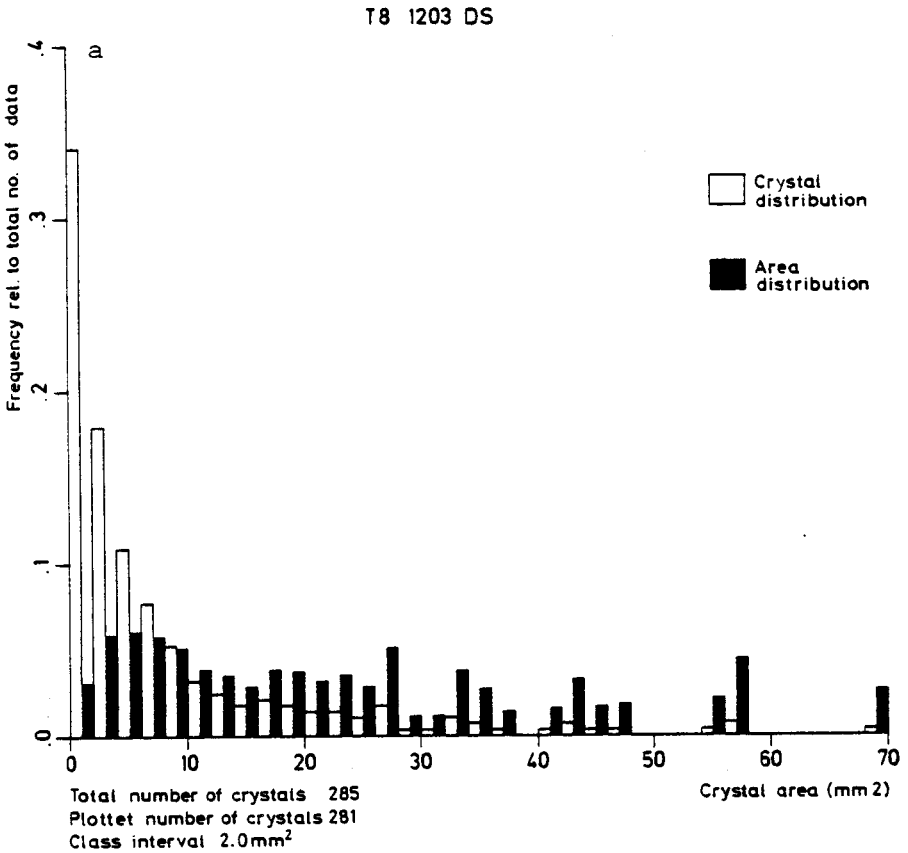

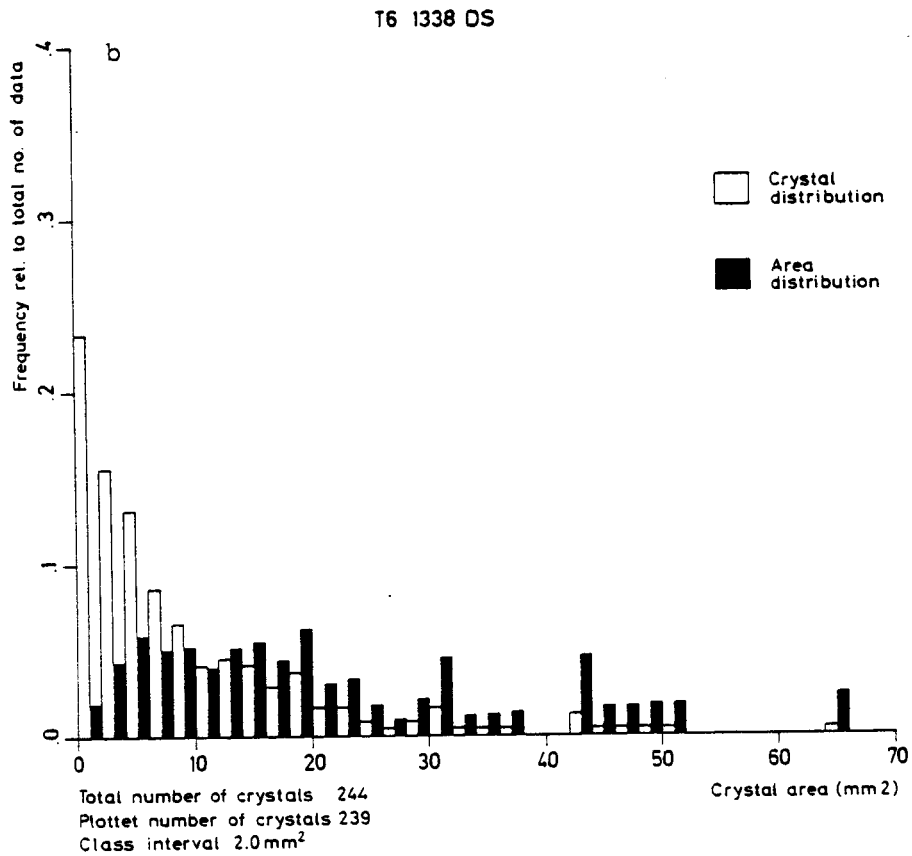

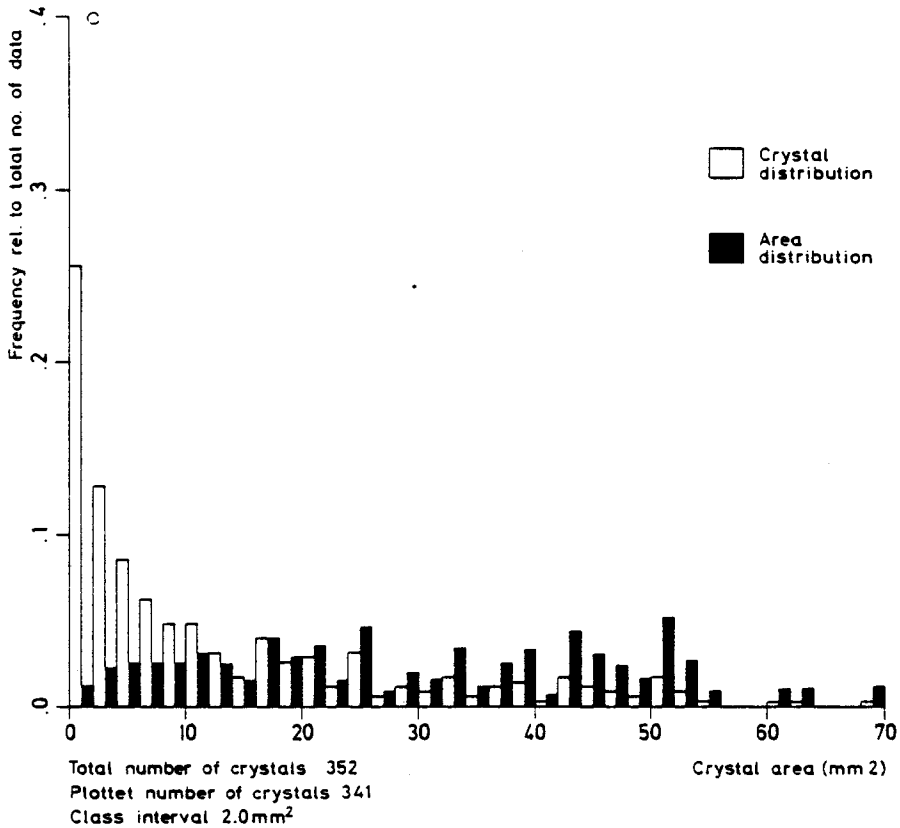

Fig. 8a-c. Frequency distribution relating relative number of crystals and their relative sum of area to crystal size in mm^2, (automated image analyses). a) areal class I; b) areal class II; c) areal class III.

heteroblastic when looked at in detail. The areal distribution can be divided into three main classes:

			symbol
I)	A narrow maximum within the interval	4-12 mm	n
II)	A broad maximum within the interval	5-20 mm	m
III)	Lack of maximum within the interval	0-50 mm	mm

The symbols to the right also visualize the distribution pattern, and the letters can be combined to illustrate the whole pattern, e.g. n, nm, ni, where a peak is represented by an i. The classification is preliminary. Table 2 summerizes the classes related to the well no. and core depth.

With the present amount of data there is no clear difference in the distribution pattern between the To-6,-8 & -9 wells.

Table 2. Classification according area distribution and grain size.

	Depth in m	I	II	III
To-5	799 DS	nm		
To-6	550 -	m		
-	860 -	nnm		
-	1022 -	nm		
-	1216 -		m	
-	1338 -		m	
-	1460 -			mm
-	1611 -			mm
To-8	760 -			mm
-	822 -			mm
-	1203 -	nm		
-	1402 -			mm
To-9	834 -	nm		
-	898 -	ni		
-	1046 -	nm		
-	1129 -			mm
-	1205 -			mm
-	1263 -			mm
-	1447 -		m	
DS:	dip section			

b. The measurements of a, b and c axes of the halite grains: As stated above these dimensions are measured on the two cut surfaces at right angle to the strike and at right angle to the dip. The longest dimension is

measured and the shortest dimension is calculated from the formula of the ellipsis.

The results from the image analyses are given in table II, appendix, together with a/c and b/c ratios, foliation dip and uniaxial compression strength. The statistical information such as standard deviation on the average values, correlation coefficient between a and c, and b and c, slope of the correlation line covariance, has not been included because they do not seem to give additional information.

Typical plot of a-c and b-c values are shown in figs. 9 a-d. These plots together with the a/c^* and b/c^* values of table II demonstrate the higher degree of flattening of the To-6 samples than those of To-8 & -9. Thus the a/c^* ratios variate between 2.3-3.1 in To-6 and 1.2-2.4 of To-8, -9 & -10 and the b/c^* ratios of To-6 range between 1.7-2.4 and between 1.0-2.0 of To -8, -9 & -10. In contrast the a/b ratios variate between 1-2 in all the wells examined showing different degree of lineation in the dip direction. The a/b - b/c^* variation is shown in

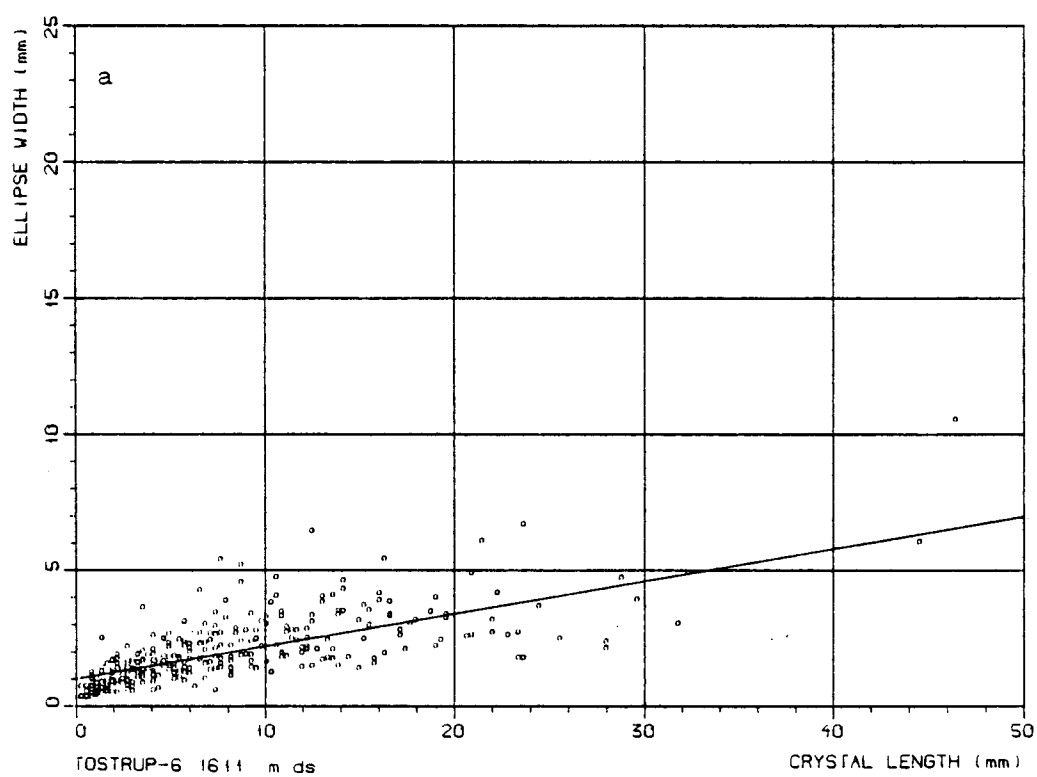

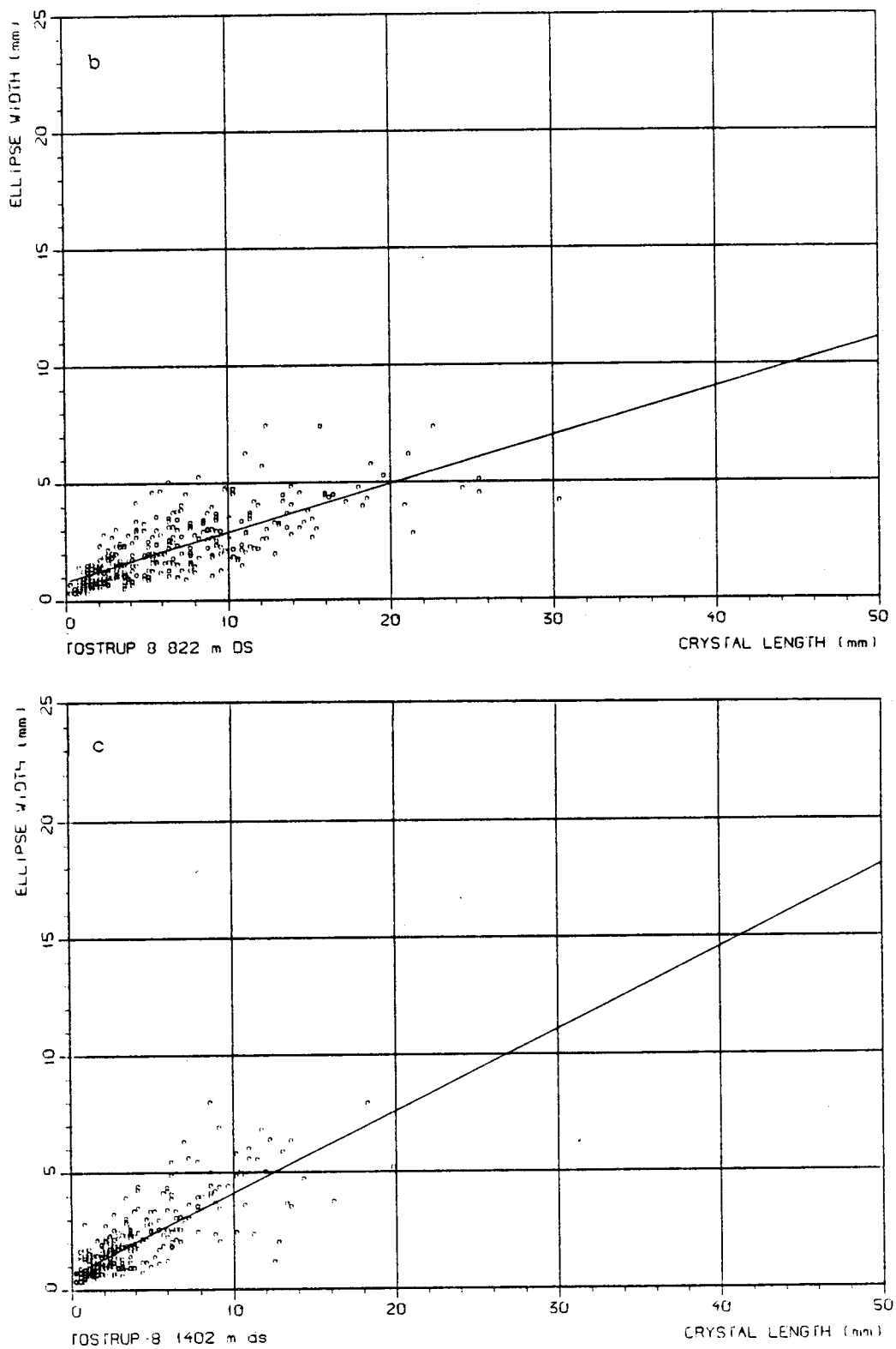

Fig. 9a-c. Representative a-c and b-c variation diagrams, (automated image analyses). a) strongly deformed Zechstein 1 rock salt; b) deformed Zechstein 2 rock salt; c) slightly deformed Zechstein 3 rock salt.

Flinn's (1962) diagram (fig. 10), which demonstrates how original cubic crystals have been deformed. Plain strain

(deformation along the a and c axes) and simple flattening are dominant deformation types, but also simple extension occurs. Thus, the rock salt is deformed under complex triaxial stress conditions.
The degree of deformation is proportional to the actual

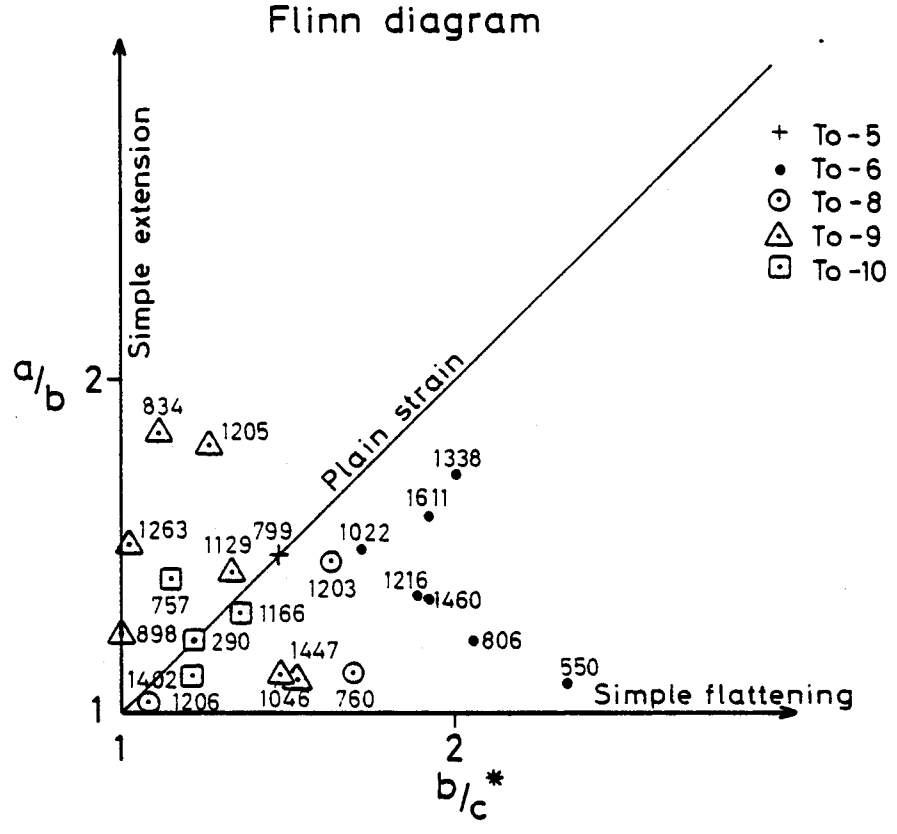

Fig. 10. Flinn (1962) diagram based on data from table II (appendix).

a/c^* ratio. A rough estimate of the degree of deformation which is recorded in the rock salt can be measured by comparison of the maximum length (a) of a grain in the dip section (DS) with the diameter of a circle of the same area (A) as the grain:

Deformation in dip section (%) = $(a\sqrt{\pi/4A} - 1)\times 100$

Using the values of table II. in To-6 the deformation ranges between 52-75% in the Z1 salt and between 21-55% in the Z2 salt of To-8,-9 & -10 whereas the Z3 salt of To-8 only show 5% deformation.

c. Form factors:

The degree of intergrowth between the halite crystals can be measured by the specific form factor (SP & SP*), perimeter/area (Underwood 1970) which shows high values for small grains and large grains with strongly interlobing boundaries. The form factor varies between 2.1-3.3 with no specific range for the To-6 salt relative to that of To-8, -9 & 10 (table 3).

Table 3. Range of the specific perimeter (SP & SP*) in sections ⊥ at the strike (DS) and ⊥ at the dip (SS).

		SP	SP*
To-6	DS	2.18-3.48	1.07-1.70
	SS	2.26-3.23	1.35-1.71
To-8	DS	2.05-3.04	1.08-1.44
	SS	2.83-3.23	1.33-1.68
To-9	DS	2.10-2.93	0.92-1.65
	SS	2.42-2.93	1.04-1.51
To-10	DS	- -	0.94-1.97
	SS	- -	1.17-1.81

SP is calculated as an average of specific form factors of individual grains
SP* is the specific perimeter calculated for average grain dimensions.

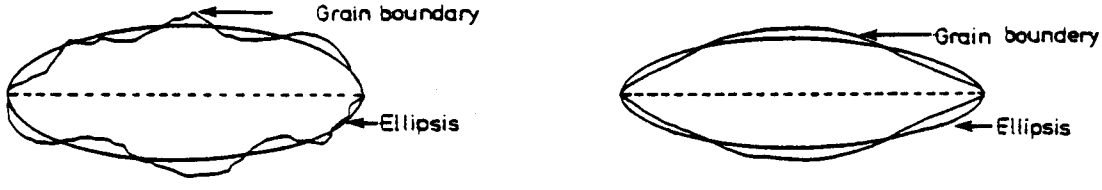

Fig. 11. Comparisons between halite grains with irregular elliptic and lensoid shapes and ellipses with the same length axis and area.

In order to quantify the degree of intergrowth independent of the grain size, an ellipsis form factor,

EFF, was designed. This factor compares the measured perimeter (P) of a grain with the perimeter of an ellipsis of the same area (A) and same a axis (fig. 11).

$$EFF = 2P/\pi(a+c) = 2aP/ (\pi a^2+4A)$$

where the shorter axis $c = 4A/\pi \cdot a$ according to the ellipsis formular $A = \pi \cdot a/2 \times c/2$. Thus EFF values above 1 show that the grain has a longer perimeter than the ellipsis which define the shortest perimeter for a given area and long axis. Typical variations related to crystal size are presented in figs. 12 a-d.
Generally the small grains, <2 mm in length, have high EFF-values, but the data on these small grains are rather uncertain due to the limited resolution of the image analyser. Grains > 2 mm tend to have lower EFF-factors. It is obvious from the frequency distribution of figs. 8 a-c that the grains < 2 mm generally form less than 5% of the analysed area, while they form more than 30% of the amount of grains. The EFF has been calculated as an average of EFF values (mean EFF) for grains >2 mm whereas the EFF* has been calculated from the average grain dimensions. In the latter case the form factor has in fact been weighed according to the grain areas so that the smaller grains count less.

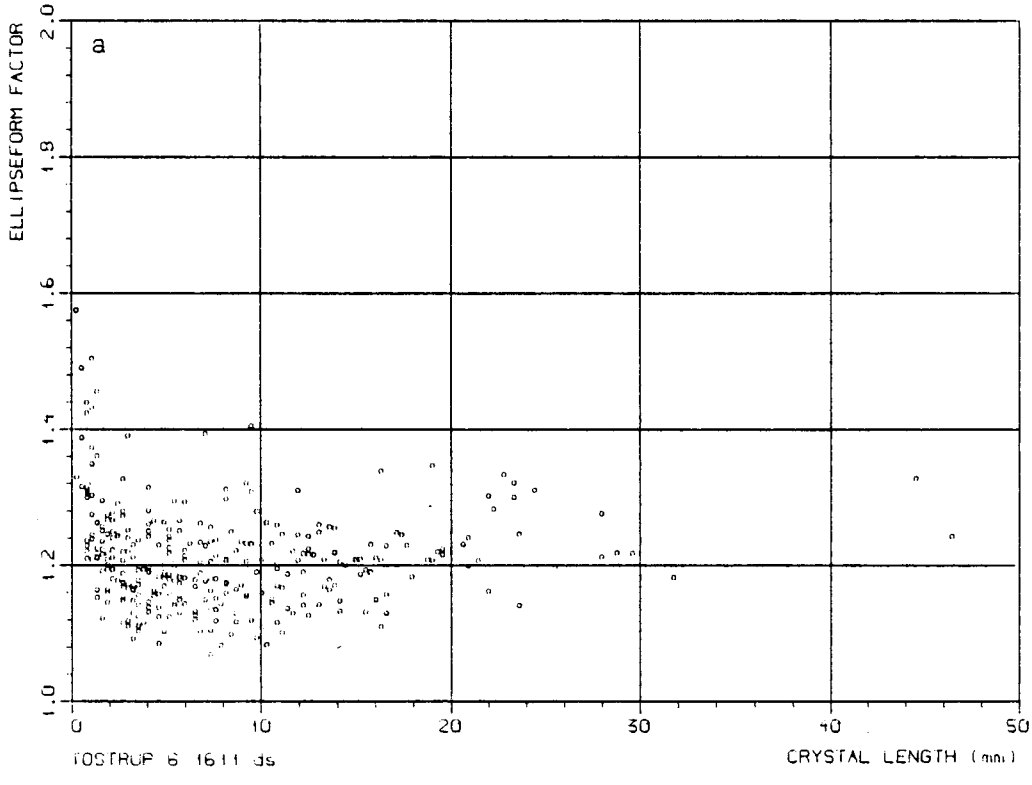

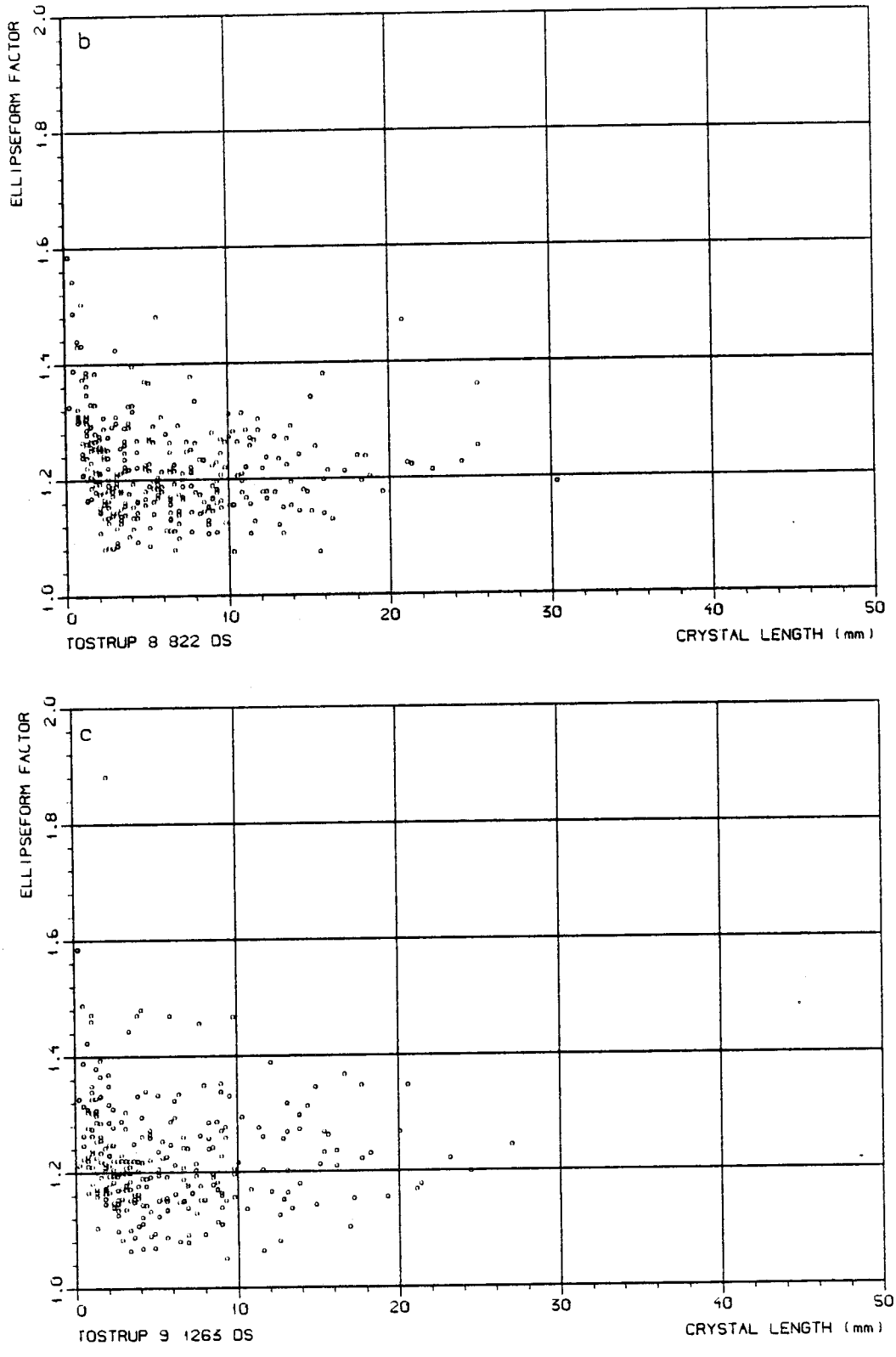

Fig. 12a-d. Representative EFF - crystal length variation diagrams, (automated image analyses). a) strongly deformed Zechstein 1 rock salt; b) deformed Zechstein 2 rock salt; c) less deformed Zechstein 2 rock salt; d) slightly deformed Zechstein 3 rock salt. Note the higher variability in the less deformed rock salt.

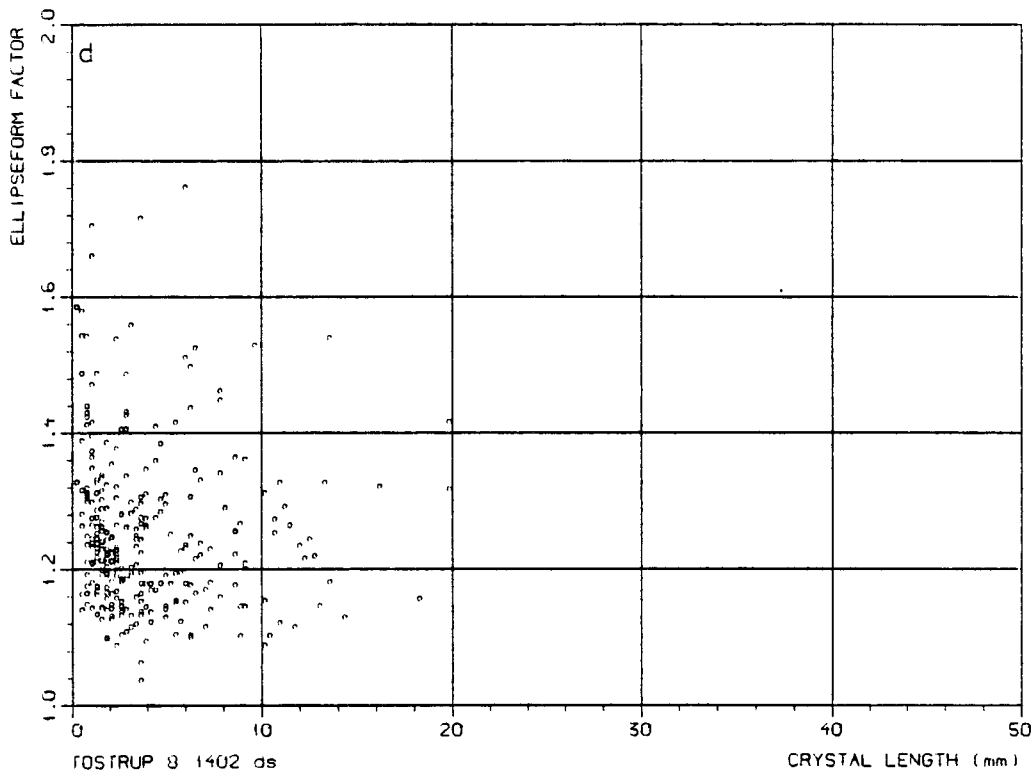

Table 4. The variation of the EFF in sections ⊥ at the strike (DS)

		Minimum values		Maximum values	
Well	Zechstein cycles	All grains	Grains >2 mm	All grains	Grains >2 mm
To-6	Z1	1.217	(1.190)	1.256	(1.222)
To-9	Z2	1.221	(1.200)	1.264	(1.226)
To-8	Z2	1.224	(1.203)	1.279	(1.241)

Table 4 shows that there is a clear overlap in the ellipsis form factor (EFF) between the rock salt of the wells. There is a scattered sympathetic relation between the EFF and SP (fig. 13), but a poor correlation between EFF* and SP* (not shown). The EFF* gives generally higher values for DS sections in the To-6 cores (table 5).

Table 5. The variation of the EFF* in section ⊥ to the strike (DS) and ⊥ to the dip (SS).

	Zechstein cycles	DS	SS
To-6:	Z1	1.094 - 1.130	1.064 - 1.108
To-8:	Z2	1.063 - 1.094	1.008 - 1.111
To-9:	Z2	1.050 - 1.111	1.005 - 1.114
To-10:	Z2	1.019 - 1.053	1.055 - 1.096

The reason for this is presumably that the shape of the grains in the To-8, -9 & -10 are closer to the ellipsoid than the strongly flattened grains of To-6. The tendency for the more flattened rock salt to obtain higher ellipsis form factors (EFF*) is shown in fig. 14. It is

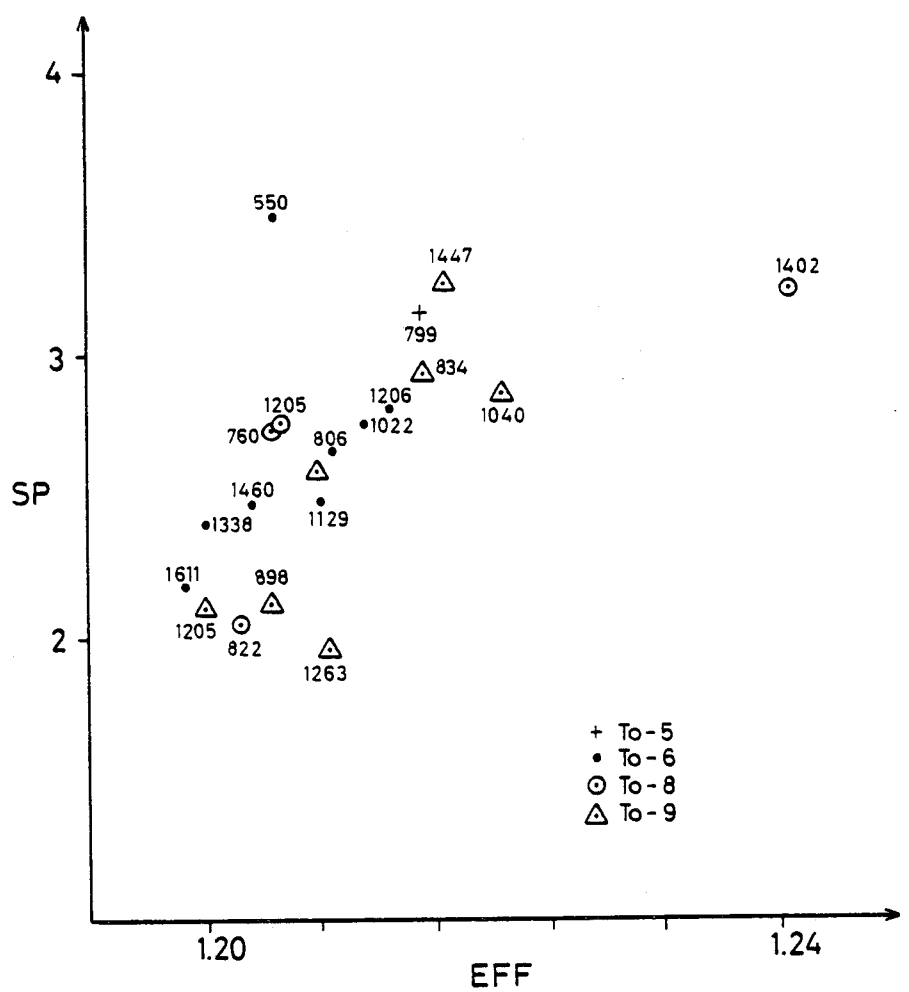

Fig. 13. Variation diagram between the ellipsis form factor EFF and the specific perimeter SP.

obvious from the replicas that the larger ellipsis form factor (EFF*) of To-6 is not due to more irregular grain boundaries, e.g. with an amoeboidal shape. The explanation seems to be, that the strongly deformed crystals are lentil-shaped and not ellipsoid-shaped.

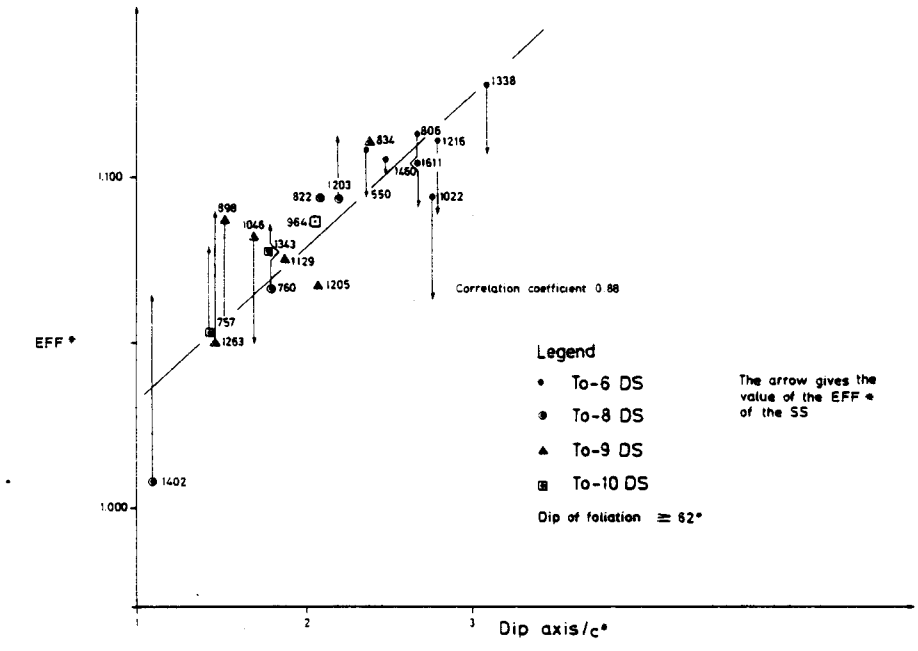

Fig. 14. Variation diagram between the dip axis/c* and the ellipsis form factor EFF* of the dip sections (DS). (Data from table I, appendix).

5. Textural analyses related to the rock mechanical strength

a.Test data: Uniaxial tests of the rock salt have been performed at the Danish Technical University (DTH) and Lehrgebiet für Unterirdisches Bauen, Hannover University (LUB-UH). The quality and significance of the test data has been evaluated by LICconsult (chapter 2.), while the present work is based on the assumption that the different methods used in the two laboratories do not significantly obscure variations due to different structures or textures of the test samples. Supporting arguments for this view is based on the test data for To-6 where both DTH and LUB-UH have been involved. Other factors originating from the drilling process and later handling of the core material may weaken the samples in different degrees. Furthermore, the textural description

has been performed on core material being situated from 0.5-4 m above or below the tested sample, and the area covered by the image analyses ranges from 63 - 126 cm . The application of the method is therefore strongly dependent on the representativeness of the samples.

b. Physical effects independent of the texture: LUB-UH (1983, fig. 6.1) has related the uniaxial compression strength to the depth of origin for To-5, -6, -7, -8, -9 and -10. The general impression from this figure is a decreasing strength of the rock salt with depth. This picture is partly due to the much higher strengths of the rock salt cored close to the salt mirror. This rock salt, however, shows textural differences, being either medium grained or slightly foliated. When these tests are ignored, there is only a significant decreasing strength with depth in To-5 and -6. Fabricius (1980) has explained this feature as a result of microfracturing due to pressure relase and contraction of the halite crystals due to temperature drop of 20-40^{o}C in the withdrawn core. In several cases stored cores produced lower strengths than those obtained immidiately after the withdrawal of the core, possibly due to the prolonged relaxation of the cores.

c. Relation between dip of foliation and uniaxial compression strength: The uniaxial strength of the rock salt combined with the geological data show that the steeply foliated samples are weaker than samples with low dipping foliation, lack of foliation or fine grain size. The fractures generated in the uniaxial tests tend to follow the foliation in samples where it is dipping more than 50^{o}. In order to show this relationship more clearly the dip of crystal foliation was measured on the tested samples where these (or good photographs) were available. Also the remaining core material was reinspected to check the relationship between the crystal foliation and bedding orientation obtained from the anhydritic bands. Figure 14 shows the relation between the dip of crystal foliation and the uniaxial compression strength:

The inverse relation between the dip of foliation and the uniaxial compression strength is obvious. The slope of the correlation line, however, is steeper for To-8,-9 & -10 than for To-3,-5,-6& -7 and the data included from the Erslev-1 & -2. The weakest rock salt in the latter two groups of wells will be around 12 MPa for vertically foliated samples, while the strongest samples, with horizontal crystal foliation have values between 25-30 MPa. In contrast the weakest samples of the former group with vertical foliation have values around 20 MPa. The very strong samples situated far to the right from the correlation line are dealt with below.

d. Relation between grain size and uniaxial compression strength: The grain size has a strong effect on the strength of the rock salt: the fine to medium grained samples have values of 23-34 MPa, and are much stronger than the coarse grained rock salt with the same dip of foliation (fig. 15a&c). In addition to the small grain size the degree of flattening is low in these rocks.

e. Relation between degree of flattening and uniaxial compression strength: The different uniaxial strengths

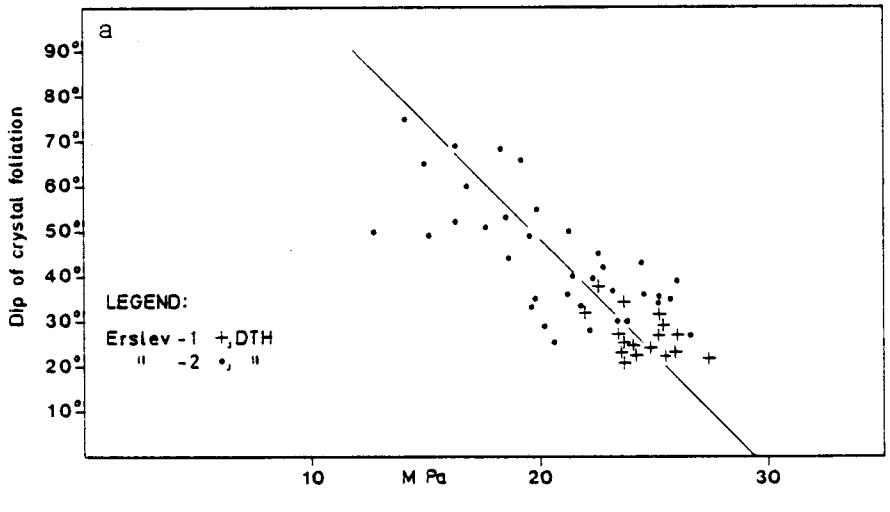

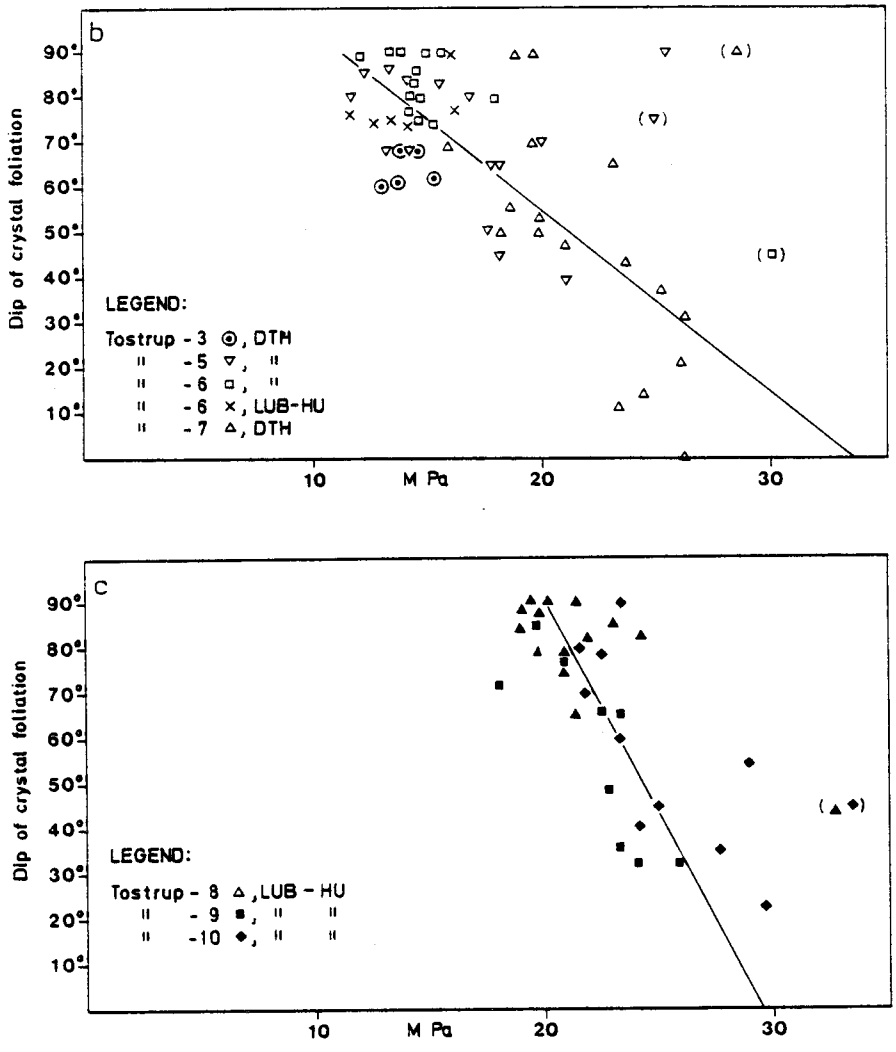

Fig. 15a-c. Dip of foliation versus uniaxial compression strength. Points in parantheses represent fine to medium grained rocks not included in the regression analysis. Linear regression gives the following results:

a. MPa intercept: 33.7; slope: -4.04; correlation coefficient: -0.79 (Three data points excluded).

b. MPa intercept: 29.4; slope:-5.15; correlation coefficient: -0.78.

c. MPa intercept: 29.7; slope:-9.43; correlation coefficient: -0.75. (Two data points above 30 MPa excluded).

of the steeply (>60^{o}) foliated rock salt from To-3, -5, -6 & -7 and To-8, -9 & -10 appear to be related to the degree of flattening, as expressed by the a/c* ratio (or dip axis/c*) as shown in fig. 16. Higher a/c* ratios correlate with lower strength values. In well foliated

rocks the foliation acts as a cleavage plane and in the uniaxial test the shear fractures follow the foliation plane when it is steeply inclined, i.e. between 0-40 relative to the direction of compression (this relation is obvious from the reports on the mechanical tests of the Tostrup rock salt). The To-9, 898 and To-8, 760 core

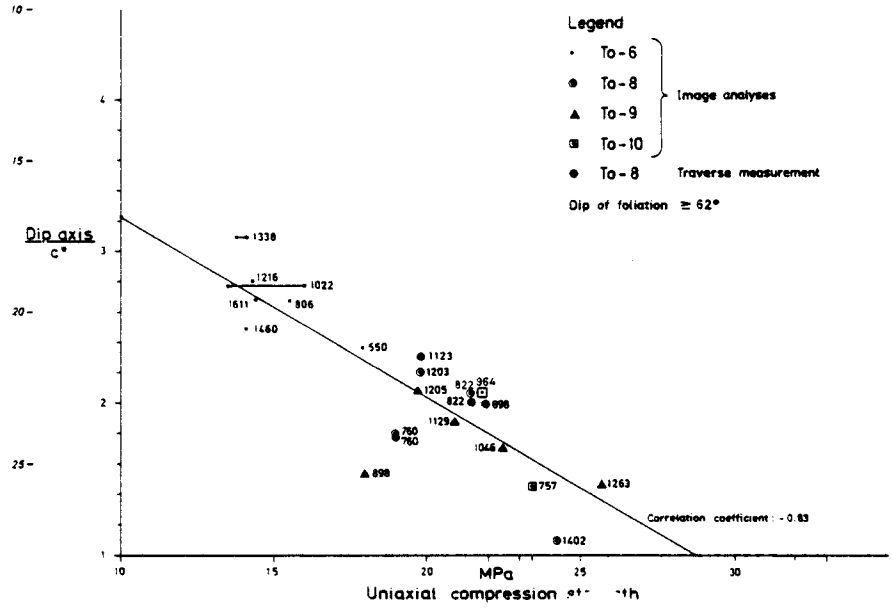

Fig. 16. Dip axis/c* versus uniaxial strength.
(Data from table I, appendix).

samples have low strengths and To-9, 834 has relatively high strength. The textural analysis indicates that both the former samples should be strong, but these analyses may not be representative for the tested ones. The high strength of To-9, 834 may be explained by textural heterogenity because the analysed sample contains alternative bands of strong and weak foliation. It should be mentioned that the a/c ratios obtained from the manual measurements of the maximum length and width of the individual grains show a large a/c scatter for the weak rock salt of To-3 & -6 and do not give a trend as that seen in fig. 15.

f. Relation between the form factors and uniaxial compression strength: Having related most of the variation of the uniaxial compression strength to the dip of crystal foliation, degree of flattening and grain

size, the form factors may only be able to explain smaller variations in the strength. There is no correlation between the form factors SP, SP* and EFF and

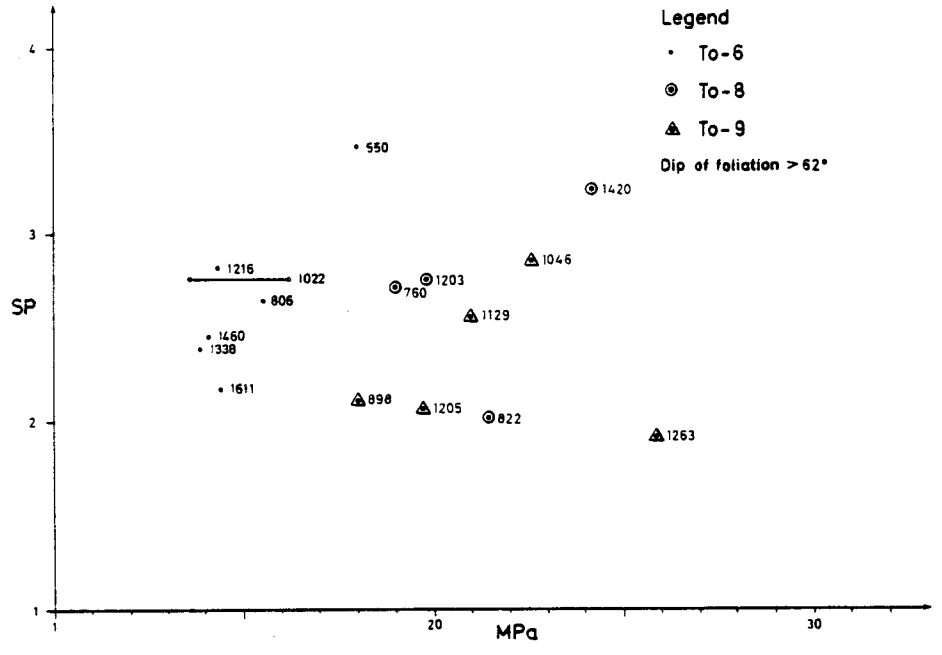

Fig 17a. Specific perimeter SP versus uniaxial compression strength. Numbers refer to depths in metres. (Data from table I, appendix).

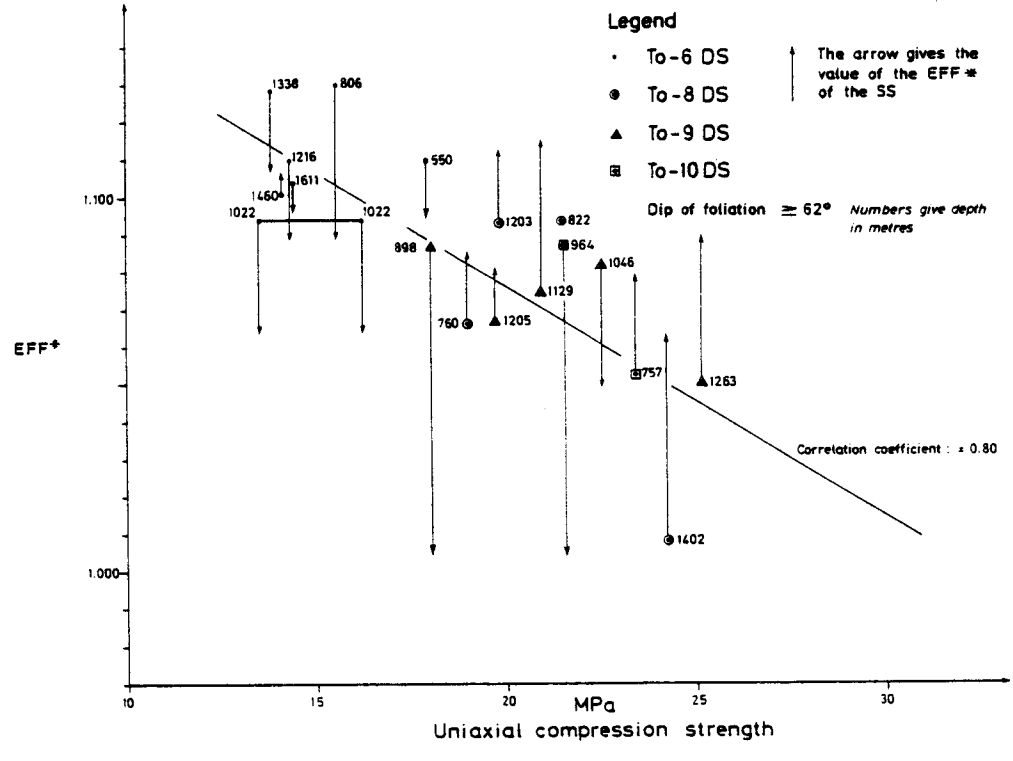

Fig. 17b. Ellipsis form factor EFF* versus uniaxial compression strength. (Data from table I, appendix).

the uniaxial strength results as exemplified in fig. 17a. There is contrary a negative correlation between the EFF* and the uniaxial strength in fig. 17b. This relation is expected because the EFF* correlates with the degree of flattening as stated on page 35.

g. Influence of the anhydrite content on the uniaxial compression strength: Anhydritic rock salt is more competent than pure rock salt and differential movements often occur at their interface. A few per cent of anhydrite appear to have produced a more competent rock which have had a drastic effect on the textures in the rock salt. In order to see whether the anhydrite content has any influence on the uniaxial compression tests the CaO content of the rock salt has been compared with the strength assuming that the CaO content is representative for the amount of anhydrite. The CaO content is taken from the chemical analyses situated closest to the mechanically tested samples. The CaO content is regarded as representative for the tested samples because the total range of ca. 10 analyses of each core is very small. The CaO content mostly variate within 0-2% and has no significant influence on the strength of the rock salt. The reason is presumably that the anhydrite content is rather low and that the anhydrite crystals are mostly situated within the halite crystals.

IV. PETROFABRIC ANALYSES.

1. Analytical methods.

a. Introduction: Petrofabric analyses of rock salt can be performed as a conventional universal stage work, but due to the coarse grained nature of the rock several thin sections have to be measured (Friedrich, 1959; Muehlenberger & Clabaugh, 1968). A special designed goniometer, has been used by Clabaugh (1962) and Clarke & Schwerdtner (1966), by which a large sample can be measured. Both these methods are slow. Generally the rocks are too coarse grained to be analysed by X-ray and

neutron diffraction methods. The present work has involved 1) conventional universal stage work together with a 2) statistical petrofabric analyses by reflection measurements on large samples. A single 3) neutron diffraction analysis has also been performed at Risø National Laboratory, but the coarse grained nature of the rock salt makes it difficult to obtain enough data points from one analysis and the result will not be delt with here.

b. Conventional petrofabric measurements: The conventional universal stage work was performed on a Wild stereomicroscope using 3-5 mm thick thin sections prepared with alcohol as a lubricant. The crystallographic orientation of the halite crystals were determined from the (100) cleavage or from the tiny cube shaped liquid inclusions. The amount of cleavages was increased significantly by shock cooling of the "thin section" in liquid nitrogen. The actual measurements were rather time consuming.

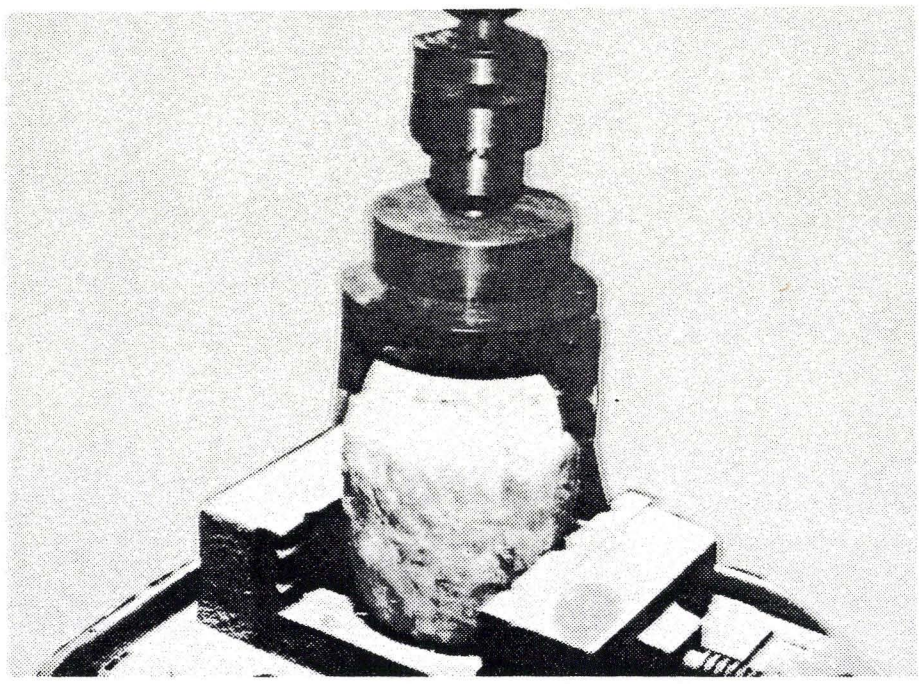

Fig. 18. Cutting of spherical rock salt samples.

c. Statistical petrofabric reflection measurements: In order to increase the amount of data, a new method, the statistic petrofabric method by reflection measurements, was developed: the samples for this type of petrofabric

analysis were half-spheres cut and grinded of the core material (fig. 18). The samples were placed in a saturated NaCl brine for several days, allowing Haüyian cubelets to grow to a size which would give bright reflections in a beam of parallel light. A spherical sample is ideal for measuring reflections in a statistical way by systematic search for reflections over an arch of more than 180°. In contrast, plane samples can only be inclined ca. 70° from horizontal if reflections are to be measured, and problems arise due to a restricted focussing range of the optical system.

In the first set up, half-spheres about 5 cm in diameter were mounted on an ordinary universal stage, using a Wild stereomicroscope (Larsen, in press).

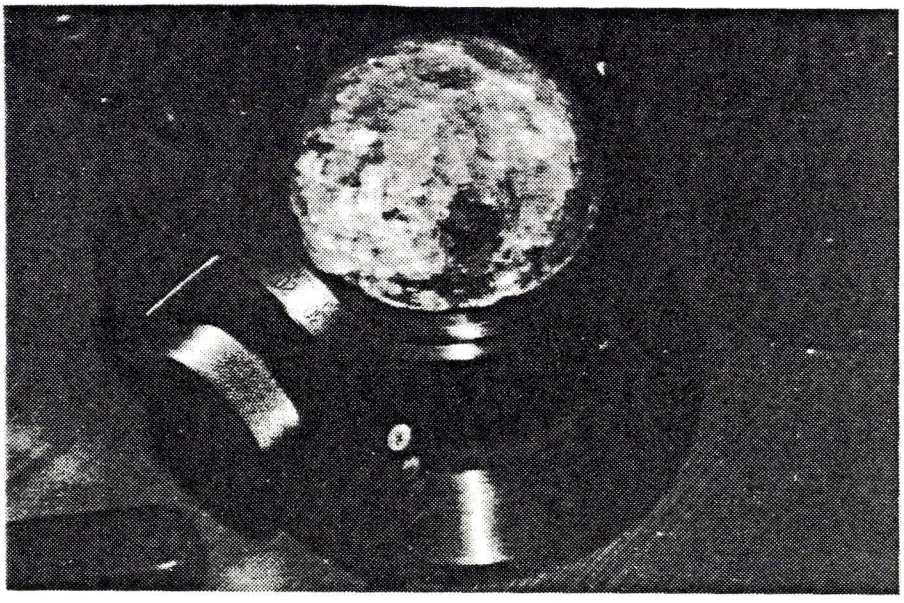

Fig. 19. The large universal stage made at the Survey. The diameter of the sphere is 10 cm.

In the second set up the sample is 10 cm in diameter and is placed on a large universal stage constructed at DGU (fig. 19). The measurements may either be performed by measuring the orientation of each crystal (generally with construction of the third face from two known) or by rotating the sample systematically at different inclinations. Grains < 2 mm in size were excluded. It is important that the measured grit is projected with even density on the Smith's net projection. This is obtained by rotating the vertical axis 360° and making

changes in the dip of this axis by stepwise rotation of 5° around the N-S axis after each rotation (fig. 20).

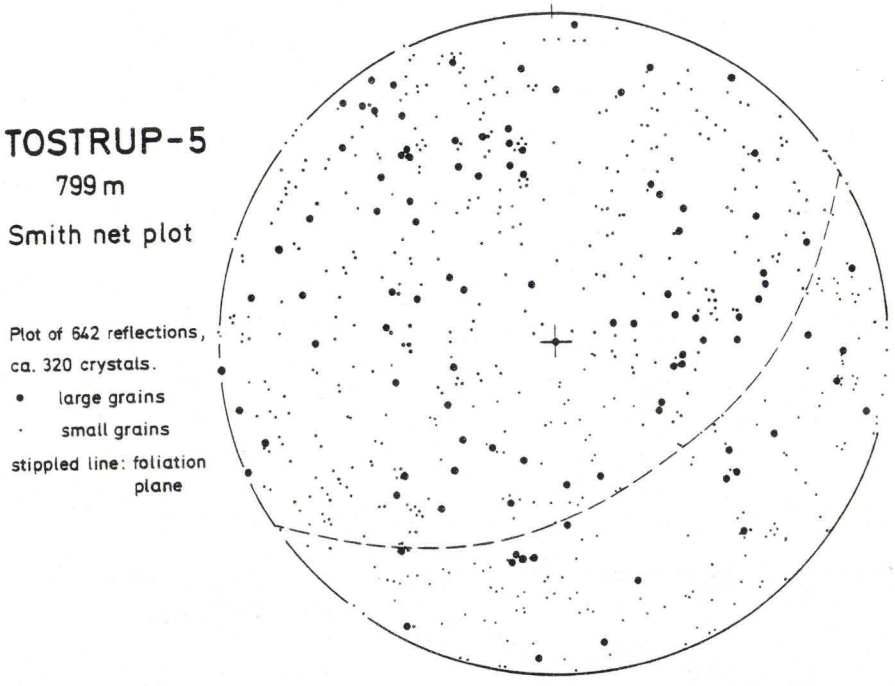

Fig. 20. An example of (100) pole reflection measurements by rotation around the vertical axis and stepwise tilting around the horizontal N-S axis. Large dots are large grains and small dots are smaller grains. (Smith's net projection).

Before the advantage of this method, however, was realized, the measurements were performed by systematic movements along the E-W- and N-S-axes i.e. the measurements followed the longitudes of the Smith's net (figs. 21A-D). Due to the convergense of the longitudes near the poles great attention is required in order to avoid repeated reflections from the same grain near the poles.

In the statistical method the number of grains in the field of view should be the same for all positions. This may be achieved by mounting an upper and lower sphere on the universal stage.

When only one half-sphere was used, measurements were performed at inclinations up to 120° from horizontal

in order to compensate for the smaller area overlooked at 90° inclination.

The measurements are plotted on a Smith's net (areal true) with a diameter of 20 cm. The contouring of the density of reflections is based on a 1 cm grit and a 1 % area counting circle as described in Hills (1963, 144-147). By this method the 1 % contour represents a random distribution.

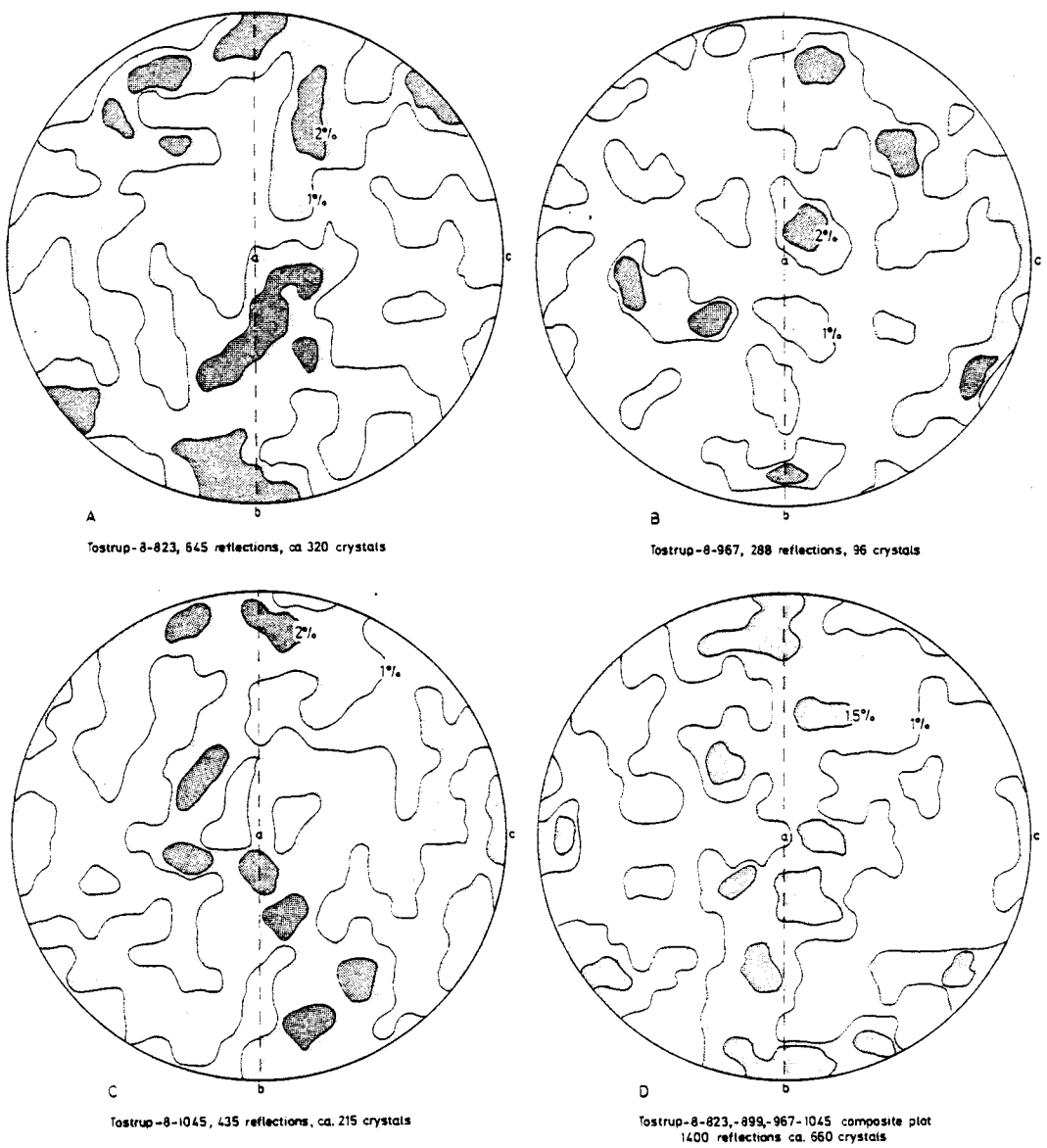

Fig. 21A-D. Fabric patterns of untested rock salt, ((100) poles). A and C by the statistical method. B by exact measurements of each crystal. D is a composite plot of A, B and C. Smith's net plot. The per cent figures give the per cent reflections of total amount of reflections within 1 per cent of the total area. Stippled line: foliation plane. a, b and c are the strain axes.

2. Analytical results of the petrofabric measurements.

a. Untested rock salt: The petrofabric patterns are shown in figs. 21 A-D. The results published are preliminary so far the figures A-D are concerned, as the statistical method was not optimized at the time they were measured (see above). Still they are believed to show the general pattern with some suppression of the concentration of reflections at 90^{o} inclination to the east and west (right and left in the fabric diagrams). The preferred orientation is relatively low, not higher than 3 % (three times higher than the 1 % random distribution). Generally the poles to the cubic faces are situated within the foliation plane, in some cases with maxima subparallel to the a axis and b axis; a maximum subparallel to the c axis is best seen in To-5, 755, the To-8 composite plot and in the To-6 composite plot (which includes uniaxial tested samples). Besides these maxima, there are maxima inclined relative to the a,.b & c axes in To-5, 799 and To-8, 823, 967 & 1045.

b. Mechanically tested samples: Fabric analyses of uniaxial and triaxial tested rock salt of To-6 were performed in order to see whether any change in crystallographic orientation has occured. Short term uniaxial tests have only been performed at room temperature with a stress rate of 1 MPa/min and a deformation at failure of 5.8-12% (at DTH). The fabric is produced as a composite plot relating the crystallographic orientation to the nearly 90^{o} dipping foliation (fig. 22A). It shows a concentration of (100) faces along the vertical foliation plane with maximum values close to the a, b and c axes (together with a pattern with only one maximum in the foliation plane). This type of fabric is similar to that of the untested foliated samples and due to low total strain no substantial change in the fabric is expected.

The triaxial tested sample was obtained from LUB-UH; the experiment took place at room temperature with a deformation rate of 0.25 %/min. until failure at a

deformation of 28.5 %. The fabric of the tested rock salt show the presence of a (100) girdle at right angle to maximum stress, , i.e. at right angle to the original foliation plane but parallel to the maximum degree of flattening. Apart from this change there is a good agreement with the position of most maxima (the maximum to the south-south-east of fig. 22A corresponds to the north-north-west maximum of fig. 22B, both being separated by ca. 30° from the foliation plane). The maximum north of the original a axis in fig. 22B has no

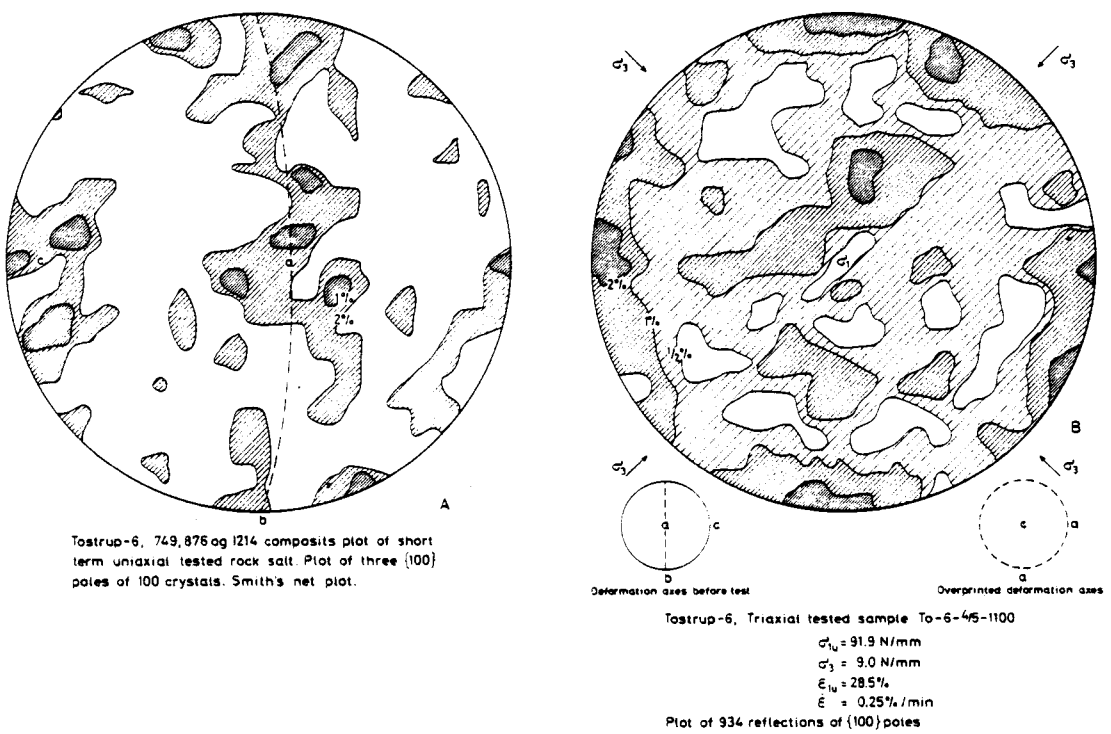

Fig 22A-B. Fabric patterns of mechanically tested rock salt. ((100) poles).
A: exact measurements of each crystal.
B: reflection measurements according to the statistical method.

certain equivalent in fig. 22A. In general, however, the original fabric has to a large extend been preserved, even though the maximum (100) pole girdle may have shiftet from a vertical to a horizontal position. This conclusion is believed to be valid in spite of the fact that the samples originate from different depths and that different petrofabric methods were used.

3. Discussion of the petrofabric data.

a. Untested rock salt: The fabric pattern of the Tostrup rock salt with two (100) pole maxima in the foliation plane and one normal to this is similar to that found in the highly folded Grand Saline dome, Texas and Winnfield, Louisiana Salt Domes (Muehlberger & Clabaugh, 1968; Schwerdtner, 1968; Carter & Hansen, 1983).

Preferred crystallographic orientation of equant grains may at low temperature be due to rotation or to internal slip with accompanying grain rotations. Under conditions where recrystallization takes place, a preferred orientation may be associated with the recrystallization process (Hobbs et al. 1976, 121-122).

According to experimental data reviewed by Carter & Hansen (1982) deformation of halite occurs along the slip systems $\{110\}\langle 1\bar{1}0\rangle$, $\{111\}\langle 1\bar{1}0\rangle$ and $\{100\}\langle 110\rangle$ (figs. 23 A-C) which are activated at increasing stress. Schwerdtner (1968), based on Dillamore and Robert's (1964) theory of preferred orientation of metals, produced a series of possible fabric patterns for translation gliding in halite. One of the patterns for very high strain is similar to the general pattern

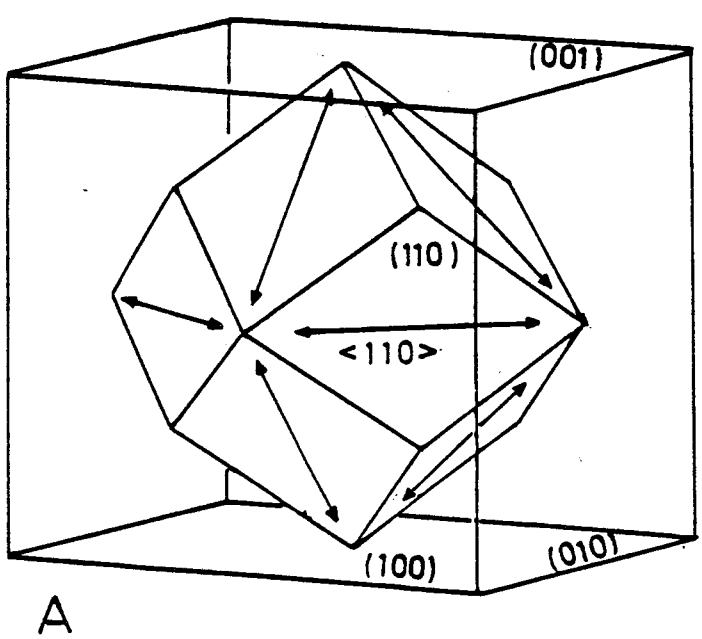

A

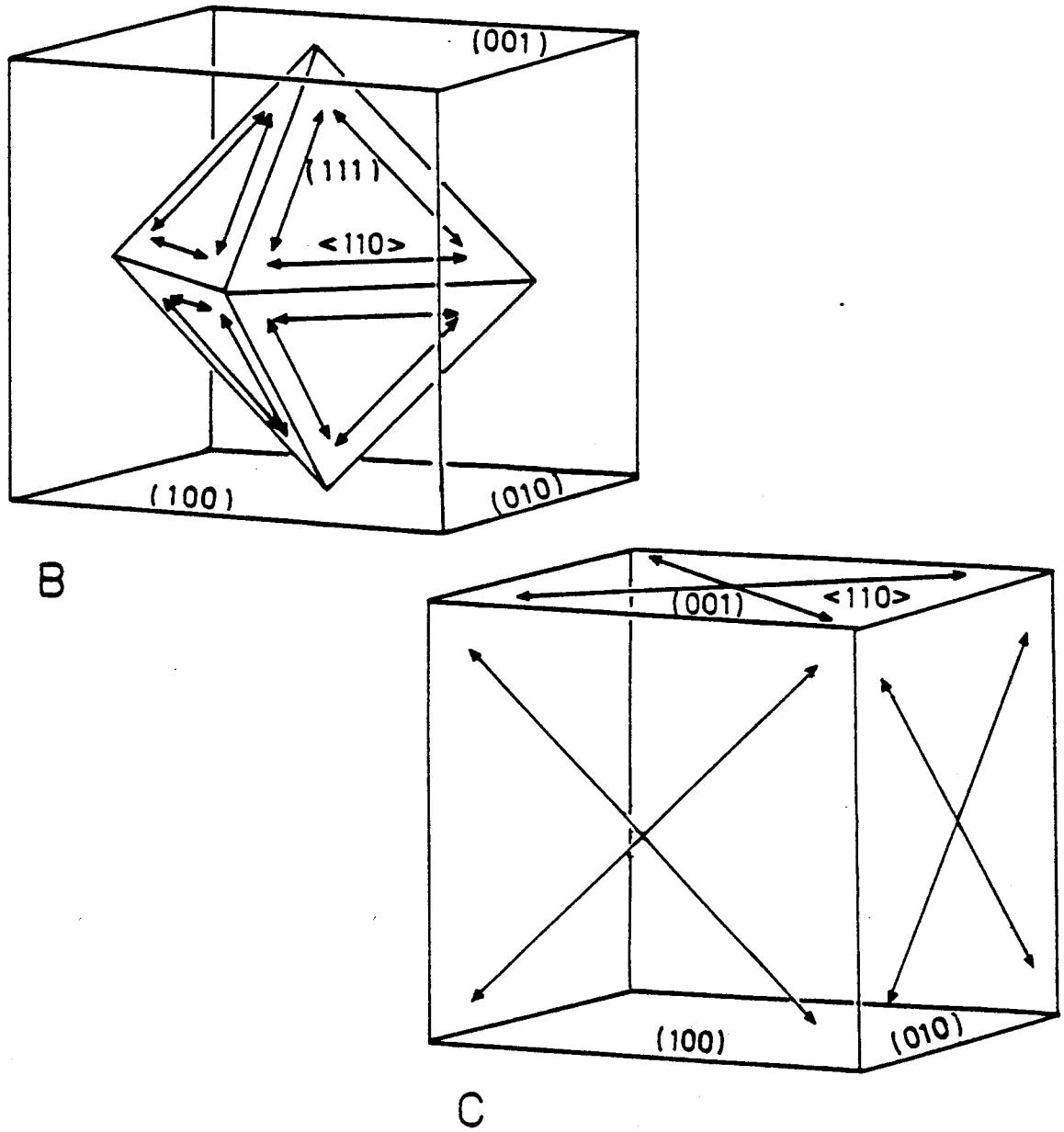

Fig. 23A-C. The gliding systems in halite.
A: {110}<1$\bar{1}$0>
B: {111}<1$\bar{1}$0>
C: {100}<110>

referred to above. But during extreme deformation the {110}<1$\bar{1}$0> slip system is expected to give a fabric pattern where the axial plane bisects the girdle between two sets of (100) pole maxima (90° apart) and intersects the third maximum (90° apart from those above) (Clabaugh, 1962). This pattern is inferred from the fact that the slip plane will tend to rotate towards the plane of maximum flattening. Schwerdtner & Morrison (1974) described highly deformed foliated and lineated rock salt from dome salt in New Brunswick showing two

diagonal (100) pole maxima, relative to the foliation plane and a third one parallel to the direction of lineation. This fabric pattern was attributed to extreme translation gliding. Experimental data on fine grained synthetic halite samples under triaxial conditions and a temperature of 100 °C produced fabric patterns, which agree with {110}<1$\bar{1}$0> gliding (Langer & Kern, 1980). Salt domes with the same fabric pattern but with equant grain shapes might have undergone annealing recrystallization according to these authors. Clabaugh (1962) and Muehlberger & Clabaugh (1968) explained their fabric analyses as a result of {100}<110> slip producing a fabric pattern with two sets of maxima (90° apart) within the foliation plane and one perpendicular to this direction. Slip along this system actually should give two maxima in the movement plane inbetween the a and b axes. A tendency to such a pattern is seen in To-5, 799. It should be noted, however, that Clarke & Schwerdtner (1966) described equant grains from slightly deformed sylvine and halite beds from ca. 1000 metres depth, whose fabric pattern shows (100) poles maxima which tend to follow the foliation plane and tend to be subparallel to the a, b and c axes. This pattern could be explained by Klamp's (1959) thermodynamic theory for competitive crystal growth under non-hydrostatic stress, i.e. syntectonic crystallization.

As stated above many of the fabric patterns contain additional (100) pole maxima situated outside the general pattern. Gliding along the {111}<1$\bar{1}$0> system is expected to produce girdles inclined 45° in relation to the c axis (i.e. outside the foliation plane). As such girdles cannot be defined the isolated maxima situated outside the planes defined by the a, b and c axes may be explained as relic fabrics, a new formed fabric due to recent differential movements or perhaps a combination of gliding along the (110) and (100) gliding planes. The second possibility of recent differential movements was favoured by Clabaugh and Muehlberger (1968) as an explanation for the poor orientation observed in the Gulf Coast salt. There was, however, no signs of discordant structures in the analysed Tostrup samples.

In general the genetic interpretation of the fabric patterns is uncertain: they may agree with the 1) Klamp's therory of syntectonic recrystallization ((100) poles coinside with the fabric axes), 2) translation gliding along the slip systems of the halite. Slip along the $\{100\}\langle 110\rangle$ slip system is not supported by experimental data as the dominant mechanism. Several mechanisms may account for oblique situated maxima and scatter of the crystallographic orientation. The data, how scarce they may be, show, that the rock salt is anisotropic and therefore may creep more easily in some directions than others.

b. Tested rock salt: It is difficult to give an explanation for the fabric of the triaxially tested rock sample but the breake up of the vertical (100) girdle could be due to slip along the $\{110\}\langle 1\bar{1}0\rangle$ slip system associated with a rotation of one of the horizontal axes. The configuration of the original fabric would favour this slip system, which is anyhow the easiest to activate at low temperature (Carter & Hansen, 1982). This slip system may have dispersed the original maximum close to the a axis. However, the formation of a horizontal maximum girdle is not explained by the $\{110\}\langle 1\bar{1}0\rangle$ slip system. Langer & Kern (1980) produced at 100 ^{o}C, a fabric with a (110) maximum parallel to the direction of maximum compression σ_1 corresponding to a (100) girdle inclined 45^{o} to σ_1 According to these experiments no horizontal (100) girdle should be expected. The well defined fabric patterns produced by these experiments are presumably due to the higher temperature.

In conclusion the fabric of the tested sample contains a strong imprint of the original fabric, but the vertical girdle of (100) faces has shifted into diffuse maxima around the direction of maximum deformation flattening, whereas a (100) pole girdle appears to have formed in the plane of maximum flattening. Thus, it may be argued that the fabric was under reconstuction in order to produce a pattern similar to the original one, i.e. with a girdle

of maxima at rigth angle to the maximum stress. The diffuse maxima around the σ_1 may be due to rotation of the grains around one of the horizontal crystallographic axes by use of the $\{110\}\langle 1\bar{1}0\rangle$ gliding system. It should be noted that the fabric does not resemble that produced by $\{110\}\langle 1\bar{1}0\rangle$ gliding in synthetic rock salt at elevated temperature (Langer & Kern, 1980). Thus the deformation mechanism in the short term compression tests at low temperature is different to that which takes place at elevated temperature and pressure at depth.

4. Relation between fabric patterns and mechanical strength.

A strong anisotropy may influence the strength of the rock salt. If the (100) faces show a maximum along the a axis in a vertically foliated rock, then vertical stress, would easily activate the $\{110\}\langle 1\bar{1}0\rangle$ gliding system, causing an early slip of grain boundaries. In the flat laying foliated rocks, a strongly anisotropic fabric (e.g. with (100) pole maxima along the a, b and c axes) may lower the strength of the rock, because the failure can occur along the vertical cleavage systems. In triaxial tests Bjørnbak-Hansen and Gravesen (1982) described failure planes of To-3 and Er-2 samples crossing steeply inclined foliation planes at a high angle whereas the rock salt with low dipping foliation showed normal failure. In both cases the failure must have followed the (100) cleavage system.

V. SIGNIFICANCE OF THE RESULTS TO THE CONSTRUCTION OF GAS CAVERNS.

The study shows that strongly deformed rock salt with textures showing vertical foliation and lineation (long axis of the halite grains being vertical) has low vertical compression strengths. Such rock salt is

expected to dominate in areas of strong diapiric upflow within the salt dome, i.e. preferentially within the central part of the salt dome. In general this rock salt is expected to belong to the older salt cycles. The low vertical compressive strength of this type of rock salt is due to a low coherence across the foliation plane caused by a low degree of intergrowth along large smooth surfaces.

Furthermore the tendency for the grains to thin out may under compression, add a wedge effect (Fabricius, 1980) by which the grain boundaries are loosened. An additional factor is the orientation of the internal gliding systems of the grains. I several cases the cubic faces tend to be subperpendicular to the strain axes. In vertically lineated rock salt this may facillitate gliding along the $\{110\}\langle 1\bar{1}0\rangle$ system and enhance the breake up of the grain boundaries. Spalling off of the cavern wall along the foliation plane is expected to occur readily at atmospheric pressure. Any fracturing, flow or fault movements are expected to occur more easily along the foliation plane and lineation direction. Conversely non-foliated, weakly foliated, low dip foliated, and fine grained rock salt have high vertical compression strengths and will give the most stable caverns under low pressure conditions. Also smaller creeping rates of these types of rock salt may be expected. LUB-UH (1983) reported lower creeping rates for the To-9 than To-6 under uniaxial tests. Under triaxial tests the creeping rates were similar.

VI. SUMMARY & CONCLUSIONS

The results of the present study include some new methods in the petrographic description of rock salt involving 1) the preparation of the samples, 2) the establishment of textural parameters and the measurement of these by automatic image analyses 3) development of a quick technic for measurement of the crystallographic

orientation of a large number of crystals, 4) correlation of the measured parameters with the mechanical strength of rock salt.

1) Due to the coarse grained nature of the rock salt, textural studies need large sections to work at. Ordinary thin sections cannot be used. For this reason a new simple and quick preparation method has been developed: The rock salt sample is cut, grinded and allowed to grow in a slightly oversaturated sodium chloride solution. The surface is reproduced on a replica where the crystal boundaries and crystallographic orientation of each crystal can be observed. For the textural analyses each crystal has been outlined with a tush pen.

2) Photo copies of the replicas have been analysed with an automatic image analyser, where maximum grain length, perimeter and area have been measured for each grain. The measured data have been used a) to characterise the rock salt by grain size and grain area frequency diagrams, b) to report strain axes and c) to calculate form factors.

a) The characterization of the rock salt by the grain size distribution has proved not to show a simple relation to the degree of deformation or the stratigraphical level, but the amount of data are restricted.

b) The strain axes measurements together with the structural analyses indicate that the a-axes (the long axis) are mostly subparallel to the dip of the foliation plane, the b-axes (intermediate axis) are subparallel to the strike of the foliation plane and the c-axes (short axis) are perpendicular to the foliation plane. With a better knowledge of the orientation of the axes in relation to the folding structure it may be possible to give a more precise structural evaluation from the core material.

The a/b and b/c ratios show that the deformation type is dominated by plain strain and simple flattening whereas simple extension is less frequent. Thus, the deformation pattern is complex.

c) Two types of form factors have been calculated: the specific perimeter (perimeter/area), SP, and the ellipsis form factor, EFF, (perimeter/calculated ellipsis perimeter) either as average for all grains or based on the average grain dimensions. The former factor, SP, gives an estimate of the surface area related to the grain volume, but this factor may give the same results for small grains, strongly flattened and strongly interlobing grain boundaries. The latter factor gives an estimate of the irregularity of the surface area from that of an ellipsis, i.e. the degree of intergrowth. The ellipsis form factor correlates with the degree of deformation, i.e. the a/c ratio showing that the factor is more dependent on the general shape of the grains than the surface irregularities. The reason is presumably that the highly deformed grains are lentile shaped rather than ellipsoide. Future work should therefore concentrate on the design of a lensoid form factor.

3) Petrofabric analyses by conventional universal stage work and by reflection measurements have been performed. The reflection measurements are done on two complementary half spheres up to 10 cm in diameter with surfaces containing regrown Haüyian cubelets. A statistical method has been introduced involving a stepwise movement of the universal stage (constructed at the institute) and a detection of reflections.
The measurements show maximum of (100) poles to be situated in the foliation plane and perpendicular to this, with a tendency for maxima to be 1) subparallel to the fabric axes a, b and c, 2) diagonal to the a and b axes and 3) situated outside the planes defined by these axes. The fabric measurements thus show, that the rock salt is structurally anisotropic.

The mechanism for the preferred orientation includes several possibilities of which recrystallization according to Klamb's (1959) theory of syntectonic crystallization (pattern 1) one of the processes and translation gliding another. It is unknown whether the oblique maxima and scatter of the crystallographic orientation may be due to translation gliding along the $\{110\}\langle 1\bar{1}0\rangle$ and the $\{100\}\langle 110\rangle$ slip system or an imprint of recent differential movements and more work is needed in order to sort out these possibilities.
The petrofabric measurement according to the reflection method makes it possible to determine the degree and orientation of strain in the individual crystals within the sample. By such measurement it may be possible to determine the gliding planes in these coarse grained rocks. Detailed work along these lines may provide information on anisotropic flow in rock salt. Furthermore petrofabric work on rock salt samples tested under relative conditions of pressure and temperatures is strongly needed in order to get a better understanding of the fabric patterns.

4) The study has shown that the compression strength of the Tostrup rock salt is related to

1. Grain size
2. Structure (dip of foliation)
3. Grain shape

whereas properties like anhydrite in small amounts and crystallographic orientation play minor roles. Fine to medium grained rock salt which occurs in the uppermost part of the salt dome has high compression strengths above 25 MPa. These rocks are exceptional at cavern depth. Among the more coarse grained rocks the grain size variation does not affect the compression strength significantly compared to the structure and grain shape. The dip of foliation related to a vertical compression shows an inverse correlation to the strength, i.e. steeply foliated rock salt shows the lowest strength

values mostly between 11-16 MPa for the To-3,-5,-6,-7. The To-3 & -5 rock salt originate from Zechstein 2 and To-6 & -7 originate from Zechstein 1 (Jacobsen, 1982). In contrast the steep dipping rock salt of To.-8,-9 & -10 show higher compression strengths of 18-22 MPa. The failure fractures are typically occuring along grain boundaries and for this reason the grain shape is an important factor.
The higher compression strength of To-8,-9,-10 correlate with a lower degree of deformation (low a/c ratio) as expressed by the ratio between the average dip axis of the grains (mostly the a-axis) and the axis perpendicular to the foliation plane (the c axis). Higher compression strength also correlate with lower ellipsis form factor, EFF*. Conversely the lower compression strength of To-6 correlates with high a/c ratios and high ellipsis form factors (EFF*). Both these features are related to the strongly flattened grains which define a pronounced foliation and cleavage plane.

Rock salt samples with more flat laying crystal foliation have high vertical compression strenths idenpendent of the degree of deformation. The strength of such rock salt is dependent on the degree of crystallographic orientation of the halite crystals, as the rupture fractures will follow the two cleavages which tend to be perpendicular to the foliation plane. Data so far obtained do not, however, indicate a strongly preferred crystallographic orientation in any examined samples and thus no great difference in the strength values is expected. It would appear that caverns constructed in strongly foliated rock salt with steep dipping foliation will show a strong tendency for spalling of the walls along the foliation plane. The agreement for this is partly that there is a low coherence across the foliation plane, partly that the lentil shaped crystals will act like wedges against each other and finally that the crystallographic orientation of the halite may facillitate translation gliding within the crystals. Any fracturing or movements will occur more easily along the foliation plane. Conversely rock salt with a low degree

of foliation, flat laying foliation and/or fine grain size is expected to be more stable.

ACKNOWLEDGMENT

Critical comments from J. Fabricius and F.L. Jacobsen at Danmarks Geologiske Undersøgelse, B. Leth Nielsen and A.K. Pedersen at Dansk Olie & Naturgas and L. Skjernaa at Geologisk Centralinstitut, University of Copenhagen have been of valuable help.

REFERENCES

Bjørnbak-Hansen J. and Gravesen, S. 1982: Triaxialforsøg med dansk stensalt, ABK report 24/81 - 1982, Technical University of Denmark.

Carter, N.L. and Hansen, F.D., 1983: Creep of rock salt. Tectonophysics, 92, p. 275-333.

Clabaugh, P.S., 1962: Petrofabric study of deformed Salt. Science, 136, p. 389-391.

Clarke, A.R. and Schwerdtner, W.M., 1966: Petrographic analysis of potash rocks at Esterhazy, Saskatchewan: Proc. 2nd Int. Symposium on Salt, p. 102-121.

Danmarks Geologiske Undersøgelse, 1982: Evaluation by the Geological Survey of Denmark of the salt dome research for radioactive waste by ELKRAFT and ELSAM, I-III, (in Danish).

Dillamore, I.L & Roberts, W.T., 1965: Preferred orientation in wrought and annealed metals. Met. Rev. 10, 271-380.

Fabricius, J., 1980: Structural analysis of core Nos. 5-9 in Geological Well Completion Report, Tostrup-5. Geological Survey of Denmark.

Fabricius, J., 1984: Formation temperature and chemistry of brine inclusions in euhedral quartz crystals from Permian salt in the Danish trough. Bull. Mineral. 107. 203-216.

Fabricius, J. in press: Studies of fluid inclusions in halite and euhedral quartz crystals from salt domes in the Norwegian-Danish basin. Proc. 6th Int. Symp. on salt.

Flinn, D., 1962: On folding during three-dimensional progressive deformation. Geol. Soc. Lond. Quart. J., 118, p. 385-433.

Friedrich, K, 1959: Gefuge und Tektonik im Hartsalz des Werragebietes. Z. deutsch. geol. Ges., 111, p. 502-524.

Gravesen, S. and Smidt, H., 1978: Compression tests of rock salt from Tostrup-3 and Hvornum: ABK report Nr. S, 24/78, Technical University of Denmark.

Gravesen, S. and Bjørnbak-Hansen, J., 1981: Short term mechanical testing of rock salt form Erslev-1: ABK report Serie S No. 44/79.1 Technical University of Denmark.

Gravesen, S. and Bjørnbak-Hansen, J., 1981: Short term mechanical testing of rock salt from Erslev-2: ABK report Serie S No. 44/79.2 Technical University of Denmark.

Gravesen, S. and Bjørnbak-Hansen, J., 1981: Short term mechanical testing of rock salt from Tostrup-5: ABK report Serie S No. 22/80.1 Technical University of Denmark.

Gravesen, S. and Bjørnbak-Hansen, J., 1981: Short term mechanical testing of rock salt from Tostrup-6: ABK report Serie S No. 29/80 Technical University of Denmark.

Gravesen, S. and Bjørnbak-Hansen, J., 1981: Short term mechanical testing of rock salt from Tostrup-7: ABK report Serie S No. 34/80 Technical University of Denmark.

Hills, E.S., 1963: Elements of Structural Geology, Methuen & Co. Ltd. London.

Hobbs, B.E. Means, W.D. and Williams, P.F., 1976: An Outline of Structural Geology, Wiley International Edition.

Institut für Unterirdisches Bauen, 1983: Gas Cavern Project Torup, rock mechanical investigations for Cavern Well To.9, DONG.

Jacobsen, F.L., 1982: Structural evaluation of the Tostrup Salt dome LL. Torup area: Internal Report, Danm. Geol. Unders.p. 1-34.

Langer, M. and Kern, H. 1980: Temperatur- und belastungsabhängiges Deformationsverhalten von Salzgesteinen. Proc. 5th Int. Symp. on Salt. p. 285-296.

Larsen. J.G., in press: New methods in textural and fabric analyses of rock salt related to mechanical test data, Tostrup salt dome, Denmark. Proc. 6th Int. Symp. on Salt.

Leffers, T., 1975: A kinematic model for plastic deformation of face-centered cubic polycrystals. Risø Report No. 302, Danish Atomic Energy Commission.

Lehrgebiet fur Unterirdisches Bauen, Universitat Hannover 1982: Gas cavern project Torup, rock mechanical study for Cavern well To-6 part 1, Laboratory tests. Preliminary results concerning the wells Tostrup 8-9-10 have been used.

Lehrgebiet für Unterirdisches Bauen, Universität Hannover, 1983: Gas Cavern Project TORUP, Rock mechanical investigations for Cavern Well TO-5.

Muehlenberger, W.R. and Clabaugh, P.S., 1968: Internal structure and petrofabrics of Gulf coast salt domes: Mem. Am. Assoc. Petrol. Geol., 8, p. 90-98.

Ottosen, N.S. & Krenk S., 1982: Mechanics of gas and oil cavities in rock salt. Bygningsstatiske Meddr. 53 No. 1. pp. 1-56.

Petersen, A.G., 1983: Salthorstkortlægning på grundlag af gravimetri kombineret med seismisk interpretation (in Danish) University of Århus, Laboratoriet for Geofysik.

Richter-Bernburg, G., 1968: Salzlagerstätten. In Geowissenschaftliche Methoden, (Bentz, A. & Martini, H.J. eds). Ferdinand Enke Verlag, Stuttgart, p. 918-1061.

Sander, B. 1930: Gefugekunde der Gesteine, Springer, Vienna.

Schwerdtner, W.M., 1968: Intergranular gliding in domal salt. Tectonophysics, 5, p. 353-381.

Schwerdtner, W.M. and Morrison, M.J., 1974: Internal-flow mechanism of salt and sylvinite in Anagance diapiric anticline near Sussex, New Brunswick. Proc. 4th Int. Symp. on Salt, p. 241-248.

Trusheim, F., 1957: Über Halokinese und ihre bedeutung für die structurelle Entwicklung Norddeutschlands. Z. Deutsch. Geol. Ges. 109, 11-151.

Underwood, E.E., 1970: Quantitative Stereology. Addison-Wesley, Cambridge Mass.

A P P E N D I X

Table I & II.

Table I Average size of strain axis as obtained from manual measurements

Well	Depth m	Type section	Dip of foliation	Long axis $\bar{a}$ m	Middle axis $\bar{b}$ mm	Short axis $\bar{c}$ mm	axis ≠ to dip	$\bar{a}/\bar{c}$	$\bar{b}/\bar{c}$	Uniaxial compression MPa
TO-3										
	1251.0	DS	68°	9.48	-	2.94	a	3.22		14.5
		SS		-	6.50	2.95			2.20	
	1359.3	DS	60°	13.08	-	3.67	a	3.56		13.0
		SS		-	9.42	5.12			1.84	
	1468.5	DS	62°	18.80		4.82	a	3.90		13.7
		SS		-	8.73	4.78			1.83	
TO-6										
	749.2	FP		7.00	5.92		a			
		DS	90°	7.24		3.21		2.26	1.91	13.6
	876.6	FP		8.70	5.86		a		1.33	
		DS	90°	8.71		4.42		1.97		14.9
	1025.6	FP		7.86	5.63					
		DS	90°	9.18		3.92	a	2.34		
		SS			5.98	3.18		2.63	1.88	13.5
	1099.6	FP		9.68	7.11					
		DS	90°	9.10		3.52	a	2.58		
		SS			6.27	3.29		2.59	1.91	14.3
	1157.0	FP	70°	13.96		3.85	a	3.63		14.4
		SS			7.61	4.02			1.89	
	1214.0	DS	70°	11.64		3.25	a	3.58		14.3
		SS			5.75	3.42			1.68	
	1380.8	FP		8.23	5.76					
		DS	75°	7.54		3.22		2.34		
		SS			6.60	3.37	a	2.80	1.96	14.4
	1458.4	FP		6.89	5.54					
		DS	90°	9.04		3.96	a	2.28		
		SS			6.59	3.90		2.10	1.69	14.2
	1612.7	FP		7.44	6.09					14.6
		DS	80°	7.87		3.66	a	2.15		
		SS			6.41	3.50		2.24	1.83	
TO-7										
	556	FP		9.06	7.17		b	1.50		23.3
		DS	0°		6.71	5.65			1.19	

Table I continued

Well	Depth m	Type section	Dip of foliation	Long axis $\bar{a}$ m	Middle axis $\bar{b}$ mm	Short axis $\bar{c}$ mm	axis ≠ to dip	$\bar{a}/\bar{c}$	$\bar{b}/\bar{c}$	Uniaxial compression MPa
To-7 cont.	822	SS		10.60		4.70	b	2.26		
		DS	21°		10.38	4.89			2.12	26.3
	946	SS		7.57		5.97	b	1.27		25.2
		DS	37°		7.02	4.24			1.66	
	1037	SS		5.49		5.25	b			23.6
		DS	44°		5.15	5.15				
	1079	DS	47°	8.19		3.44	a	2.38		21.0
		SS			5.59	3.61			1.55	
	1246	DS	58°	12.64		4.07	a	3.11		18.6
		SS			5.74	4.08			1.41	
	1252	DS	53°	13.27		3.97	a	3.34		18.6
		SS			7.29	4.66			1.56	
	1289	DS	14°	9.50		3.58	a	2.65		24.4
		SS			7.57	3.94		1.92		
	1341	SS		9.24		5.44	b	1.70		19.9
		DS	50°		8.48	5.24			1.62	
	1349	SS		9.29		5.56	b	1.67		19.9
		DS	53°		7.55	4.50			1.68	
	1505	DS	90°	7.74		4.88	a	1.59		17.8
		SS			6.73	4.53			1.50	
	1741	DS	69°	13.91		4.63	a	3.00		15.9
		SS			9.70	4.50			2.16	
Er-1										
	1248	DS	19°	12.76		5.71	a	2.23		25.4
		SS			8.13	5.36			1.52	
	1252	DS	19°	11.79		5.17	a	2.28		24.0
		SS			8.96	5.22			1.72	
	1253	DS	25°	10.88		4.25	a	2.56		24.0
		SS			8.95	5.25			1.70	
	1263	DS	26°	12.01		3.94	a	3.05		25.0
		SS			7.57	3.46			2.19	
	1284	DS	17°	11.63		3.65	a	3.19		
		SS			9.13	4.69			1.99	

Table I continued

Well	Depth m	Type section	Dip of foliation	Long axis $\bar{a}$ m	Middle axis $\bar{b}$ mm	Short axis $\bar{c}$ mm	axis ≠ to dip	$\bar{a}/\bar{c}$	$\bar{b}/\bar{c}$	Uniaxial compression MPa
Er-1 cont.	1293	DS	23°	15.98		5.29	a	3.02		25.5
		SS			8.48	4.37			1.94	
	1301	DS	19°	13.67		6.01	a	2.27		25.9
		SS			10.08	5.66			1.79	
Er-2										
	1284	DS	28°	10.12		4.69	a	2.16		20.0
		SS			8.45	5.05			1.67	
	2273	DS	46°	8.76		3.70	a	2.37		19.9
		SS			6.56	2.28			2.88	
	2855	DS	40°	8.84		3.79	a	2.33		21.8
		SS			7.72	3.50			2.21	

Legend:

FP = Section parallel to the foliation plane

SS = Section ⊥ to the dip direction

DS = Section ⊥ to the strike

$\bar{a}$, $\bar{b}$ & $\bar{c}$ = average from individual measurements. The standard deviation show a range of 50-100% relative on these average values.

TABLE II

Well no.	Io-5		Io-6										Io-6 continued										Io-8			
Depth (m)		799.5	550.7		806.0		1022.0		1216.5		1338.4		1460.9		1611.0		760.3		822.7		1203.7			1402.9		
Type of section	SS	DS	SS	DS	DS	SS	DS	SS	DS	SS	DS	SS	DS	SS	DS	SS	DS	SS	DS		DS	SS	SS	DS		
Dip of foliation		53°		80°	90°		90°		79°		75°		77°		73°		84°		90°		79°			80-85°		
A, area (mm^2)	11.05	6.25	7.41	6.33	9.59	8.47	10.51	7.84	9.97	8.17	11.20	5.96	11.71	8.20	16.77	9.21	10.35	8.95	14.58		9.15	5.86	6.95	7.73		
P, perimeter (mm)	12.82	9.62	11.56	10.77	13.93	11.99	14.23	10.95	14.10	11.60	15.56	10.18	14.78	11.81	18.02	12.44	12.69	11.90	15.80		12.64	9.82	10.01	9.95		
a, long axis (mm)	4.96		4.72		5.72		6.08		5.96		6.64		6.01		7.56		4.88		6.20		5.06		3.37			
b, middle axis (mm)		3.43		4.32		4.70		4.13		4.44		3.91		4.47		4.75		4.39				3.49		3.29		
c* } short axes	2.84	2.32	2.00	1.86	2.14	2.29	2.20	2.41	2.13	2.35	2.15	1.94	2.45	2.34	2.82	2.47	2.70	2.60	2.99		2.30	2.14	2.63	2.99		
č } short axes	1.73	1.22	1.33	1.24	1.57	1.58	1.45	1.58	1.44	1.64	1.59	1.48	1.68	1.77	1.92	1.88	1.78	1.83	2.13		1.57	1.53	1.76	1.78		
axis ≠ to dip	b		b		a		a		a		a		a		a		a		-		a		b			
a/c*	1.75		2.36		2.67		2.77		2.80		3.08		2.45		2.68		1.80		2.07		2.20		1.28			
a/č	2.87		3.55		3.64		4.19		4.14		4.18		3.58		3.94		2.74		2.91		3.22		1.91			
b/c*		1.48		2.32		2.05		1.72		1.89		2.01		1.91		1.92		1.70				1.63		1.10		
b/č		2.81		3.48		2.97		2.61		2.71		2.68		2.53		2.53		2.40				2.28		1.85		
a/b	1.45		1.09		1.22		1.47		1.34		1.70		1.34		1.59		1.11		-		1.45		1.02			
EFF*	1.047	1.065	1.095	1.108	1.130	1.091	1.094	1.064	1.110	1.089	1.128	1.108	1.102	1.105	1.164	1.097	1.066	1.084	1.094		1.093	1.111	1.063	1.008		
Eff	1.214	1.219	1.211	1.222	1.211	1.208	1.202	1.214	1.216	1.209	1.200	1.202	1.204	1.204	1.198	1.190	1.212	1.338	1.203		1.207	1.234	1.235	1.241		
SP* mm^{-1}	1.16	1.54	1.56	1.70	1.45	1.42	1.35	1.40	1.41	1.42	1.39	1.71	1.26	1.44	1.07	1.35	1.23	1.33	1.08		1.38	1.68	1.44	1.29		
SP mm^{-1}	2.64	3.15	3.23	3.48	2.66	2.86	2.75	2.96	2.81	2.70	2.40	3.02	2.47	2.45	2.18	2.26	2.72	2.83	2.06		2.76	3.19	3.04	3.23		
Uniaxial compression strength MPa	20.0		17.9		15.5		13.5	16.1+	14.3		13.8	14.1+	14.1		14.4		19.0+		21.4+		19.8+		24.2+			
Depth of tested sample (m)	798.6		552.3		805.4		1025.6	1024	1214.1		1337.0	1341	1458.4		1612.7		761		823		1202		1400			

Legend:

DS: Cut section at right angle to the strike of the crystal foliation

SS: Cut section at right angle to the dip direction of the crystal foliation

A: Average grain area in cut sections

P: Average grain perimeter in cut sections

a: Average long grain axis projected onto the general dip direction

b: Average middle grain axis projected onto the general strike direction

c*: Average short grain axis calculated as the ellipsis width of the average grain dimension

č: Average short grain axis calculated as an average of calculated individual ellipsis widths from each sample

EFF*: Ellipsis form factor defined by the average perimeter P divided by the perimeter $\frac{\pi}{2}(a+c^*)$ based on average grain dimensions.

Eff: Ellipsis form factor calculated as average of the Eff_i for all grains > 2 mm.

SP*: Average specific perimeter defined as, P/A, for average values of P_i and A_i from individual grains

Legend continued:

SP: Average specific perimeter defined as average of P_i/A_i for all grains

The uniaxial compression strength data either originate from DTH or from LUB-UH (marked with a +)

Well no.	To-9														To-10										
Depth (m)	834.4		898.6		1046.8		1129.5		1205.0		1263.0			1447.0	290.5		757.7		964.6		1166.1		1206.5		1343
Type of section	DS	SS	DS	SS	DS	SS	DS	SS	DS	SS	DS	SS	SS	DS	SS	DS	DS	SS	DS	SS	DS	SS	DS	SS	DS
Dip of foliation	49°		62°		66°		77°		85°		83°			15°		45°	90°		70°		35°		23°		
A, area (mm^2)	12.29	7.85	11.075	11.70	8.72	8.13	10.52	7.40	15.80	8.02	17.10	10.96	6.26	6.55	4.00	4.31	16.35	10.67	9.19	5.57	11.07	7.82	10.19	9.35	6.22
P, perimeter (mm)	15.16	10.45	13.109	12.19	11.72	10.81	12.98	10.86	16.05	10.91	15.67	12.78	10.36	9.88	7.86	7.78	15.36	12.51	12.46	8.42	12.62	10.72	11.67	11.49	9.93
a, long axis (mm)	6.13		4.65		4.34		5.02		6.47		5.65		3.97		2.63		5.49		4.92		4.80		4.20		3.74
b, middle axis (mm)		3.35		3.84		3.91		3.55		3.60		3.79		3.57		2.54		3.95		2.53		3.68		3.81	
c* (short axes)	2.55	2.99	3.03	3.88	2.56	2.64	2.67	2.65	3.11	2.83	3.86	3.68	2.01	2.34	1.94	2.16	3.79	3.44	2.38	2.81	2.94	2.70	3.09	3.13	2.12
c̄ (short axes)	1.72	1.87	2.26	2.35	1.72	1.65	1.77	1.97	2.04	2.06	2.56	2.70	1.42	1.63	1.35	1.32	2.44	2.48	1.61	1.33	1.84	1.86	1.89	1.99	1.28
axis ⊥ to dip	a		a		a		a		a		a		b		b		a		a		a		a		
a/c*	2.40		1.53		1.70		1.88		2.08		1.47		1.98		1.36		1.45		2.07		1.63		1.36		1.77
a/c̄	3.56		2.06		2.52		2.84		3.17		2.21		2.80		1.95		2.25		3.06		2.61		2.22		2.92
b/c*		1.12		0.99		1.48		1.34		1.27		1.03		1.53		1.18		1.15		0.90		1.36		1.22	
b/c̄		1.79		1.63		2.37		1.80		1.75		1.40		2.19		1.93		1.59		1.90		1.98		1.91	
a/b	1.83		1.21		1.11		1.41		1.80		1.49		1.11		1.17		1.39		1.94		1.30		1.10		
Eff*	1.111	1.050	1.087	1.005	1.082	1.050	1.075	1.114	1.067	1.079	1.050	1.089	1.103	1.066	1.096	1.053	1.053	1.078	1.087	1.005	1.039	1.069	1.019	1.055	1.080
Eff	1.219	1.262	1.206	1.230	1.226	1.225	1.210	1.245	1.205	1.220	1.211	1.242	1.221	1.205											
SP* mm^{-1}	1.23	1.33	1.18	1.04	1.34	1.33	1.23	1.47	1.02	1.36	0.92	1.17	1.65	1.51	1.97	1.81	0.94	1.17	1.36	1.51	1.74	1.37	1.15	1.23	1.60
SP mm^{-1}	2.53	2.93	2.13	2.42	2.86	3.08	2.59	2.59	2.10	2.45	1.96	2.11	3.25	3.00											
Uniaxial compression strength MPa	22.8+		18.0+		22.5+	18.3+	20.9+		19.7+		25.7+	24.6*		-	33.5+		23.4+		21.7+		27.7+		29.6+		
Depth of tested sample (m)	835.3		901.0		1048.6	1041	1130.2		1204.3		1257.2	1258			290		756		963		1162		1205		

CHAPTER 2.

STATISTICAL ANALYSIS OF MECHANICAL PROPERTIES OF ROCK SALT

By Per Lagoni

LICconsult

CONTENTS

STATISTICAL ANALYSIS OF MECHANICAL PROPERTIES OF ROCK SALT

1. INTRODUCTION

This report presents the work undertaken by LICconsult on statistical analysis of the mechanical properties of rock salt.

The work is a part of a major salt research project managed by Geological Survey of Denmark. The purpose of this project is to improve the understanding of the internal structure, the mineralogical composition and the rock mechanical properties of Danish salt domes, cf. ref. /1/.

The purpose of the present part of the project is to evaluate practical applications of advanced statistical methods in the analysis of petrographical and rockmechanical properties of the salt.

The Danish energy agency - DEA, a public authority supervising and approving industrial applications of salt domes in Denmark, issued in 1982 a set of guidelines for the design and construction of leached caverns to be used for natural gas storage, cf. ref. /2/.

The guidelines recommend a systematic application of a variety of data in the assessment of the mechanical properties of the salt surrounding a cavern;

- geological classification of salt samples

- borehole logging and

- mechanical testing of samples.

The international experience and practice, dominated by German, English, French and American experts, do not provide any unique or unified method of handling these data.

The experience gained in Denmark during the design of D.O.N.G.'s natural gas cavern plant in Ll. Torup, ref. /3/ - a work which has been followed closely by LICconsult as a consultant to DEA - clearly demonstrates the need for new engineering methods in the process of concentrating the huge amount of data into characteristical design parameters.

An important contribution to this development has been produced by Jørgen Gutzon Larsen in another part of the above research project, cf. ref. /4/. Gutzon Larsen has introduced new methods in textural and fabric analysis of rock salt allowing quantification of the micro structure of the salt. The data produced by Larsen are considered very important in this project.

The methodology, data and results of LICconsult's work are shortly summarized in section 2.

The analytical methods included are outlined and discussed in section 3 and further detailed in section 5.

The analytical - mostly empirical - models necessary for more refined analysis are dealt with in section 4.

The salt data applied, the data sources and the quantity as well as quality of data are described in section 6.

Finally, the results obtained and a thorough discussion of these are presented in section 7 and 8.

2. SUMMARY

Through a systematic evaluation of various statistical methods using a data base of salt data from the Tostrup Salt Dome, two methods have been selected as appropriate for investigation of rock mechanical properties of salt.

For a qualitative evaluation of large amounts of different types of data, f.ex.

- strength
- creep strain
- texture and
- various logs

the correlation analysis, providing either simple or partial correlation coefficients between pairs of salt parameters, seems to be useful.

However, the correlation analysis does not provide any qualitative results concerning salt properties. It therefore mainly serves as a tool in the initial phase of evaluation of the possible applications of a specific data base.

Simple linear regression analysis are generally not sufficient, because of the very complex behaviour of salt.

For the objective preparation of a design basis for a rockmechanical design of caverns in a salt dome, a general nonlinear regression analysis seems to be required.

As a result of the present project a series of interesting relations between salt strength and various structural parameters or log results is presented. It is demonstrated that even for a relatively poor data base - poor because of missing/insufficient information for the individual salt samples - the general regression analysis

provides a systematic objective method to extract rock mechanical design data, primarily shear strength of the salt, from the various salt data available.

In principle, the method provides the necessary objective tool to extrapolate rockmechanical data from the small amount of tested samples to the entire salt mass influenced by a cavern.

Within this project it has not been the intension to do so, but the possibilities are certainly open.

3. ANALYTICAL METHODS. INTRODUCTION

The purpose of an analysis of salt to be used in the design of cavities in a salt dome, is to provide a set of characteristic relations between rock stresses and strains at various stress levels, temperatures, etc.

A general approach to this problem aiming at a complete description and understanding of all processes involved is not practicable.

Within the limits of this project the following empirical approach has been adopted - an approach which in our experience leads to reasonable and useful results in rock and soil mechanics;

- a few, characteristic parameters describing the mechanical properties of the salt are selected, f.ex. shear strength and creep rate

- various parameters influencing these parameters are selected f.ex. stress history, temperature, salt fabric texture

- empirical relations between parameters are defined, with due consideration of theoretical bonds, and qualitative experience.

Introducing the synonyms

Y_i for characteristic mechanical parameters

X_j for typical, usually independent parameters and

F_K for empirical realtions between Y and X

we may formulate the stated problems as a set of equations

$$
\begin{aligned}
Y_1 &= F_1 (X_1, X_2, \ldots, X_n) \\
Y_2 &= F_2 (X_1, X_2, \ldots, X_n) \qquad (1) \\
- \quad &- \quad - \\
- \quad &- \quad -
\end{aligned}
$$

The main purpose of the present work has been to establish methods able to

- point out important parameters influencing a certain mechanical parameter, i.e. the X_i ´s in each of the equations (1)

- provide estimates of empirical relations between mechanical parameters and basic parameters, i.e. the mathematical form of (1)

- to provide estimates of empirical parameters in the equations (1).

If methods exists that are able to fulfil this purpose, an important goal is reached: The possibility of predicting mechanical properties by means of substituting physical properties and conditions in the salt.

Before further details in the analytical method are introduced in section 5, the following section 4 will discuss the parameters and empirical relations introduced above.

4. SALT PARAMETERS AND MATERIAL MODELS

Characteristic Mechanical Parameters

Based on the international experience and to a certain extent controlled by available data the following parameters have been selected which characterize mechanical properties of the salt:

$\frac{1}{2}(\sigma_1-\sigma_3)$ = shear stress applied in a uniaxial or triaxial test rig (either σ_1 or σ_3 = constant)

E = tangent modulus

ν = Poisson ratio

ε = axial strain component measured in uniaxial or triaxial test rig.

Of specific interest is the maximum value of $\frac{1}{2}(\sigma_1-\sigma_3)$ in a short therm test (the short term shear strength), E at very low stress levels (the initial slope E_i of the stress-strain curve σ_1 versus ε_1), ε corresponding to the short term shear strength (ε_{1f}) and ε at fixed time intervals after load change $\Delta(\sigma_1-\sigma_3)_{creep}$ in a creep test.

The parameters used are defined in figure 1 and 2.

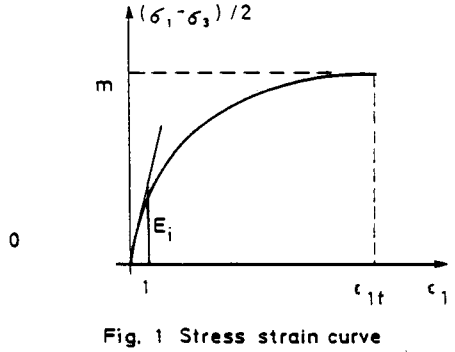

Fig. 1 Stress strain curve

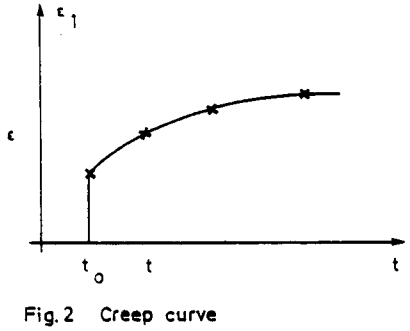

Fig. 2 Creep curve

Parameters

As for the mechanical parameters a set of typical basic parameters has been selected, simply from experience

$1/2\ (\sigma_1+\sigma_3)$ = mean stress applied in a uniaxial or triaxial test rig

t = time since load change

δ = dip of foliation (angle to vertical which is generally also the direction of σ_L in mechanical tests)

EFF = crystal shape parameter introduced in ref. /4/, cf. also section 7

a/c* = crystal shape parameter introduced in ref. /4/ cf. also section 7

N = compensated neutron log value (%)

ΔD = borehole size, deviation from ideal diameter (caliper log result)

γ = gammy ray log value (API units)

ρ = bulk density (g/cm^3).

From experience, see fx. ref. /5/, we know that test results depend on the test procedure which is different in different laboratories. This dependence is taken into account too. Other equally important factors, such as temperature and test strain rate, are not considered, as they are kept constant in the data base available.

Empirical Models of Rock Salt Behaviour

Material Models

As a result of many years of rockmechanical research in the behaviour of rock salts, a variety of material models has been developed and verified, mainly against uniaxial and triaxial, short and long term, creep and failure

tests, ref. /5/, which gives an excellent overview of the status of rock mechanics for salt.

Three different types of material models are generally applied more or less independent of each other:

- failure conditions providing the relation between stress components in a state of failure, f.ex. the Mohr Coulomb failure condition, which for a triaxial state of stress $\sigma_1 > \sigma_2 = \sigma_3$ reads

$$\sigma_1 - \sigma_3 = 2 \cdot c \cdot \cos\phi + (\sigma_1 + \sigma_3)\sin\phi \qquad (2)$$

  The cohesion c and the friction angle normally depends on the stress level.

- constitutive laws providing the relation between the state of stress and the time independent strains, f..ex. Hooke's law, where the modulus of elasticity E normally is assumed to decrease with increasing shear stresses (non-linear elastic behaviour). For a triaxial state of stress the main equation with respect to interpretation of laboratory tests is

$$\varepsilon_1 = \frac{1}{E}(\sigma_1 - 2\nu\sigma_3)$$

  Poissons ratio is normally assumed constant corresponding to incompressibility of the salt ($\nu = 0.5$).

- creep laws providing the relation between the state of stress, the stress-time history and the strains in the salt material, f.ex. Menzel-Schreiners or Burgers creep law.

$$\Delta\varepsilon_1 = A \cdot \Delta(\sigma_1 - \sigma_3)^n (t - t_o)^m \qquad \text{Menzel-Schreiner} \quad (4)$$

$$\Delta\varepsilon_1 = \left(\frac{(t - t_0)}{\bar{\eta}_M} - \exp\left(-\bar{E}_K (t - t_0)/\bar{\eta}_K\right)/\bar{E}_K \right) \Delta(\sigma_1 - \sigma_3)$$

$$\text{Burger (linear)} \quad (5)$$

were A, n, m, $\bar{\eta}_M$, $\bar{\eta}_K$ and $\bar{E}_K$ are creep parameters and t_o is the time for the (momentary) stress change $\Delta(\sigma_1 - \sigma_3)$

Traditionally, the creep parameters are constants for a specific salt sample but in some cases $\bar{\eta}_M$, $\bar{\eta}_K$ and $\bar{E}_K$ are assumed stress dependent (f.ex. the modified Burger law applied in the Tostrup design).

The choise of material models for the present study mainly depends on a subjective preference rather than rational arguments. The main purpose is not to document one material model being better than others, rather to use the material models as a necessary tool to provide a qualitative bond between stresses, strains and time in order to be able to disclose the correlation between petrografical properties of the salt and the mechanical behaviour. From the same arguments we do not need to use very complicated mathematical models.

The question, which material model is the best in various situations, is still interesting but the answer has to be given in another context.

Influence of Non-mechanical Salt Characteristics

Only limited research has been conducted within the area of relating non-mechanical salt characteristics (petrographical data and log data) to mechanical salt characteristics (strength, stiffness). One important contribution already mentioned, is the work by Gutzon Larsen, Ref. /4/.

To our knowledge, no sophisticated relations have been proposed earlier and therefore we assume simple linear relations between selected petrographical data and each parameter in the material laws.

Analytical Formulation of Material Models

The actual models applied in the project are selected on the basis outlined in the previous section:

- the Mohr Coulomb failure condition, equation (2) with a modification often used in soil mechanics, cf. ref. /6/

$$\sin\phi = b^* \cdot (\sigma_1 + \sigma_3)^d \qquad (6)$$

- a time-independent constitutive law also used in soil mechanics

$$\sigma_1 - \sigma_3 = \frac{E_i \ \varepsilon_1}{\left(1 + \frac{\varepsilon_1}{\varepsilon_{1f}(a-1)}\right)^a} \quad \text{for } \varepsilon_1 \leq \varepsilon_{1f} \qquad (7)$$

  This model reflects linear elasticity at very low stress levels

$$\sigma_1 - \sigma_3 \simeq E_i \cdot \varepsilon_1, \quad \text{cf. equation (3)} \qquad (8)$$

  and ideal plasticity at failure ($\varepsilon_1 = \varepsilon_{1f}$)

- a time dependent creep law of the Menzel-Schreiner type, cf. equation (4), which is sufficiently accurate for the present purpose.

The empirical constants in the models above are all assumed to be linear functions of the parameters introduced at page 82 e.g. the cohesion in the Mohr Coulomb failure condition

$$c = c_0 + c_1\delta + c_2 \cdot EFF + c_3 \cdot (a/c^*) + c_4 \cdot n + c_5 \cdot \Delta D + c_6\gamma + c_7\rho$$

or expressed in matrix notation

$$\begin{bmatrix} b \\ c \\ d \\ A \\ m \\ n \\ E \\ a \end{bmatrix} = \begin{bmatrix} b_o \\ c_o \\ \\ \\ \\ \\ \\ a_o \end{bmatrix} + \begin{bmatrix} b_1 \text{ --- } b_7 \\ c_1 \text{ --- } \\ \\ \\ \\ \\ \\ a_7 \end{bmatrix} \begin{bmatrix} \delta \\ EFF \\ (a/c)^* \\ n \\ \Delta D \\ \gamma \\ \rho \\ \end{bmatrix}$$

Immediately, it might seem unrealistic to describe the salt behaviour by means of 56 constants. However, this is not the intention, but before a closer explanation is given, the analytical method adopted will be clarified in more details.

5. ANALYTICAL METHOD; DETAILED DESCRIPTION

Statistical Methods

Different statistical tools exist, especially fitted for analysis of test data, f.ex.

- analysis of variance and co-variance
- linear regressions analysis
- correlation analysis
- general regression analysis

For the analysis of a test data base of more or less random origin, most of these tools are useless.

Analysis of variance or co-variance normally requires esperiments under full control or completely random selection of the most significant test factors and test conditions.

In problems of the present type with a rather limited data base, a biased selection of groups of test conditions and a significant amount of incomplete

"observations", the analysis of variance and co-variance appears to be less efficient.

The linear regression analysis provides some possibilities but in general the non-liniarities in salt behaviour are too significant to allow a liniarization, cf. section 4 For the analysis of the influence of a single factor, eg. a structural parameter, on a single property, eg. the uniaxial shear strength, the liniar regression analysis proves efficient, cf. ref. /4/. However, the possibility of extending or combining various analyses is actually limited.

Left in the list of tools is the correlation analysis and the general regression analysis, which have been used extensively in this project and therefore deserves a more comprehensive discussion.

Correlation Analysis

The correlation analysis provides a simple statistical measure of the dependency among various properties.

The square of the correlation coefficient r_{ij} between two variables X_i and X_j (property or parameter) estimates the fraction of the variance of X_i accounted for by the variation of X_j.

Considering all combinations (i, j) - in this case all combinations of characteristic salt properties as defined earlier - we are - based on r_{ij} - able to test statistically the dependency between pairs of parameters and point out any significant correlation, which deserves closer analysis.

However, if many parameters are mutually correlated, r_{ij} is not sufficient to make this decission.

Instead, we have to determine the partial correlation coefficients $r_{ijkl\cdots m}$, which estimates the fraction of the variance of X_j accounted for by the variation of X_j when the effect of the variation of any other parameters $X_{kj}, \ldots, X_m$ has been removed.

General Regression Analysis

The introduction to analytical methods, section 3, described the basic problem to be solved by means of the general regression analysis i.e. the determination of empirical constants in funktions relating various properties of the salt to the shear strength and the creep behaviour.

The regression analysis is performed in the following steps:

a. A subroutine to the general regression program LIC70 is prepared calculating the shear strength $\frac{1}{2}(\sigma_1-\sigma_3)$ and the axial strain in a creep test from

   - the models defined at page 85-86

   - salt characteristics and log results as defined at page 85-86

   - a set of empirical constants

b. From the data base, observations are selected, i.e. groups of data related to each individual sample. For the present study a subset of the complete data base characterized by a maximum distance Δd (within the same well) of 100 m between the sample tested mechanically and the nearest sample, which has been analysed structurally.

c. Each observation is given a statistical weight

   $W = (\Delta d-2)^{-\frac{1}{2}}$ for $d \geq 2$ m

   $W = 1.0$ for $d \geq 2$ m

   $W = 0.0$ if significant data are missing in an observation.

The major advantage of LIC70 analysis is that the statistical information in a data base is utilized completely even if the basic physical/mathematical model is very complex and the data base is very in-complete.

d. The weight function is chosen on a qualitative basis only, as no detailed information can be extracted from the data base.

e. A series of interactive analysis has been performed with the purposes:

- to identify properties having a significant influence on the mechanical properties of salt

- to estimate empirical constants including a test origin factor f_o which takes the value 1.0 for shear strength test made at LUB, cf. page..., and a value determined by the regression analysis for test made at ABK. The reason for this origin factor is a recognized dependency of the different test procedures used at the two laboratories, cf. ref. /5/. f_o is multiplied on the shear strength $(\sigma_1-\sigma_3)$ calculated from equation (2).

f. A final analysis based on the experience gained from step e, which provides:

- best estimates of significant empirical constants

- the standard deviation of each constant

- the statistics of the complete regression analysis, i.e. correlation coefficient and standard deviation of $(\sigma_1-\sigma_3)$ and creep strains when estimated from structural properties etc.

6. DATA SOURCES

The salt data base collected as a part of the project, entirely consists of results from the Tostrup gas storage project.

Different sources supplied data to the storage project. These data are in general made available to this project by D.O.N.G. A/S.

For pratical reasons only data directly available from the following sources have been included in the data base:

- D.O.N.G. A/S — Well Completion reports, Tostrup 5, 6 and 7. (logs digitized by LICconsult)
- LUB — Rockmechanical Investigation Tostrup 5, 6, 7, 8, 9 and 10 (tables and curves digitized by LICconsult)
- DGU — Data used for the preparation of ref. /4/ (tables)
- ABK — Short term uniaxial tests and uniaxial creep tests (tables and raw data)

Further, extensions of the data base, f.ex. additional wells, material test raw data etc, are of course possible, but outside the scope of work.

Main emphasize has been put on results from salt samples with the majority of data present, i.e.

- short term shear strength (uniaxial or triaxial)
- creep data

- fabric and texture data and

- log results

It is impossible to obtain a data base of reasonable size of all data should be available for each sample.

Fortunately, the analytical method applied, provides facilities to account for missing data or data of varying significance, cf. the weighing procedure described above.

7. RESULTS

Correlation Analysis

The numerical results of the correlation analysis performed are summarized in this section.

The presentation only includes a small part of the results produced. As an example, the results from a complete correlation analysis of a single subset of observations including 19 variables comprises 19 mean values, 19 standard deviation, (19+20)2 = 190 cross correlation coefficients, 190 simple regression coefficients and at least 190 partial correlation coefficients.

By means of statistical tests, significant correlations have been extracted. To limit the total analysis only the most significant correlations have been included in the presentation and in the regression analysis presented later.

Figure 3 shows for the most significant structural properties (a/c*, EFF and foliation dip δ , cf. section 4), the simple correlation coefficient r between the uniaxial shear strength $1/2(\sigma_1 - \sigma_3)$ and these parameters.

The critical value of r for an equal tail test of the hypothesis r = 0 is also shown.

The following conclusions are made from fig. 3.:

- r tends to decrease with increasing distance Δd between the sample tested mechanicaly and the sample analyzed structurally, but no significant drop is noted for $\Delta d \leq 50$ m approximately.

- In physical terms, this result indicates that the limit of extrapolation of salt properties measured in a certain location in the salt dome is approximately 50 to 100 m in a vertical

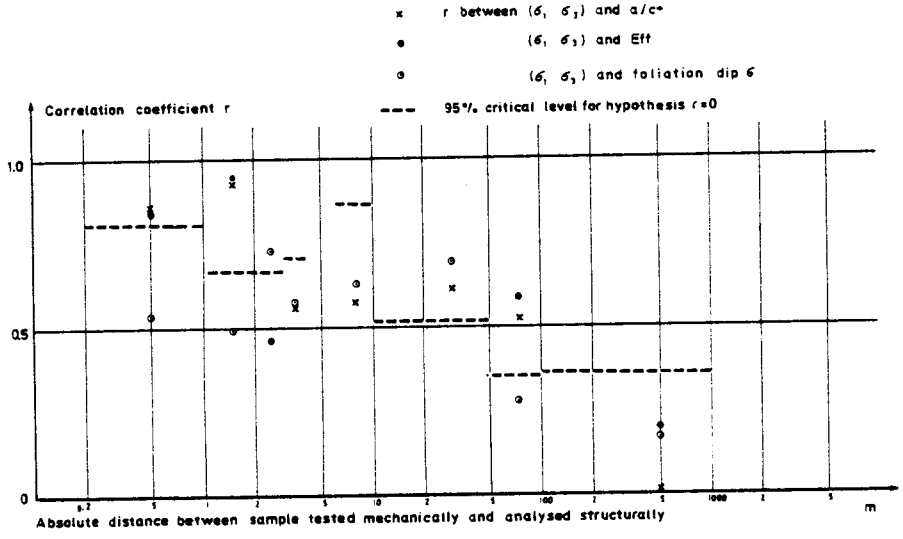

Fig. 3. Correlation coefficient between uniaxial strength and structural parameters.

direction. Unfortunately the data base does not provide data to make a similar conclusion concerning horizontal extrapolation.

- The structural parameters EFF and a/c* tends to have a more significant influence on strength than the dip of foliation which in turn is more significant than other structural parameters determined in ref. /4/, i.e. the same conclusion as reached by Gutzon Larsen.

Table I shows the partial correlation coefficients between the shear strength $1/2\ (\sigma_1 - \sigma_3)$ and any of the parameters analysed. The results are based on tests with $\Delta d < 100$ m.

Parameter	no.of obs	Partial correlation coefficient r	Critical value 95% level	Significantly $\neq 0$
E_i	98	0.72	0.22	yes
dip	98	-0.09	0.22	no
A_{DS}	96	-0.17	0.23	no
A_{SS}	100	-0.18	0.22	no
P_{DS}	96	-0.48	0.22	yes
P_{SS}	100	-0.41	0.22	yes
a	96	-0.54	0.23	yes
b	100	-0.58	0.22	yes
c^*_{DS}	96	0.24	0.23	yes
c^*_{SS}	100	0.26	0.22	yes
$\bar{c}_{DS}$	96	0.12	0.23	no
$\bar{c}_{SS}$	97	0.15	0.23	no
a/c	96	-0.43	0.22	yes
Eff	96	-0.53	0.22	yes
GRL γ	68	0.53	0.28	yes
CAL ΔD	67	-0.13	0.28	no
DEN ρ	68	-0.05	0.28	no
CNL N	20	0.42	0.28	yes

Table I clearly shows where to look for significant parameters correlated with shear strength (uniaxial and triaxial).

As one would expect, there is a significant positive correlation to the stiffness parameter E_i , see figure 1.

Among the structural parameters, the most significant correlation is found to the length of the crystal axes (a, b and c), to the average crystal perimeter P and to the derived shape parameters.

$$EFF = 2P/\pi(a+c) \quad \text{and} \quad a/c^*$$

The latter ones have been used further on. The correlation coefficients are positive which means that elongated crystals are supposed to give smaller strength than "spherical" crystals.

Contrary to the work of Gutzon Larsen (only involving uniaxial shear strength), the present analysis (uniaxial and triaxial strength) shows no correlation between strength and dip of foliation. This result supports the findings at LUB showing less or no influence of the dip on triaxial strength.

Small values on the gamma ray and density logs show significant positive correlation to the strength.
The gamma ray log reflects a.o. the potassium content of the salt and increasing gamma ray values mean increasing potassium content and increasing strenth of the salt.

The explanation for this relation is more a change to another and stronger structure than strength of the potassium minerals. The density log reflects the density of the rock salt. Increasing density values mean increasing strength of the salt too. This relation is correlated to the content of anhydrite crystallized as disseminated small crystals, which stabilize the rock salt.

Regression Analysis

The results of the correlation analysis demonstrates the fact that no quantitative results are obtained which are applicable for design purposes.

However, such results are produced from the general regression analysis and presented in this section.

The analysis also provides some qualitative results concerning the composition and the content of information in the data base:

- the number of complete observations, i.e. data from mechanical and structural tests and logs related to the same sample is very limited (approx. 15 tests)

- the total number of observations is 119.

- the total number of strength tests supported by structural tests and logs is 92 with a total weight of 59.4, cf. page 88-89.

- the total number of creep tests supported by structural tests and logs is 22 with a total weight of 16.3.

Although the data base has a significant number of entires, we must conclude that the basis for analysis of creep behaviour of salt is insufficient and some reservations must be attached to the results concerning salt strength.

Despite of this, all analyses have been conducted to the extent possible, merely to illustrate the possibilities of the method employed.

Due to the fact that structural data are not specifically related to the individual samples tested mechanically (which is the case for log results) the analysis has been separated into two, one investigating mechanical properties versus structural parameters and one investigating mechanical properties versus log data.

Salt Strength versus Salt Structure

From the total analysis, the following results are obtained concerning the short term shear strength of Tostrup salt, cf. the basic model described in section 4:

The best estimate of the friction angle ϕ is calculated from

$$\sin\phi = b \cdot (\sigma_1 + \sigma_3)^d$$

where

$$b = 0.39+0.043\cdot(a/c^*) + 0.37\cdot EFF$$

$$d = -0.059 -0.0066\cdot(a/c^*)$$

The best estimate of the cohesion c is calculated from

$$c = f_o \cdot (4.1-0.6\ (a/c^*)-1.2 \cdot EFF)\ (MPa)$$

where

f_o = 1.0 for LUB tests
1.03 for ABK tests

Only contributions with a significant statistical influence on the shear strength have been included on the basis of the general regression analysis.

The correlation coefficient for the regression analysis is 0.996, which means that 99.6% of the variance of the ultimate shear strength $(\sigma_1-\sigma_3)$ is explained by the variations in the structural parameters a/c*, EFF and ρ the test origin factor f_o and the mean stress $(\sigma_1+\sigma_3)$ in the samples.

The standard deviation of the shear strength estimated from these parameters is 0.88 MPa.

It is rather difficult to illustrate the measured versus the estimated shear strength because of the multi parameter variations.

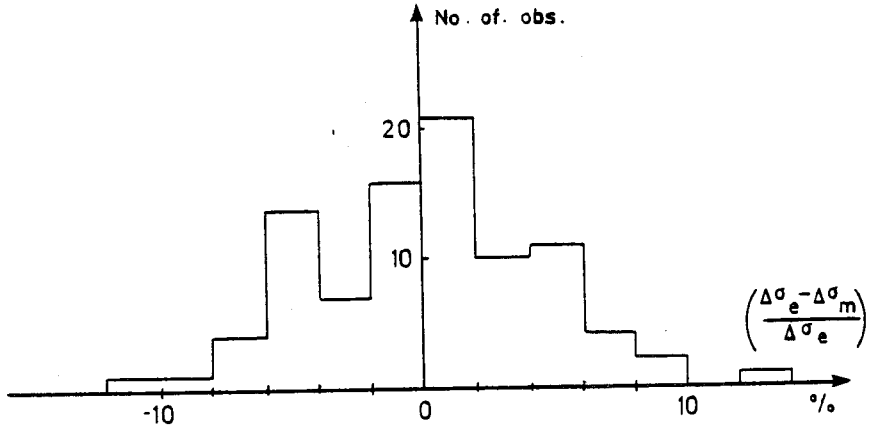

Figure 4 shows the distribution of the relative difference between measured and estimated shear strength from all tests (with weight >0) involved in the analysis.

Salt Strength versus Log Results

Instead of relating the salt strength to structural parameters, which suffer from the fact that they are not directly related to the same samples as strength data, the log results from four logs have been used.

The following results are obtained concerning friction angle ϕ and cohession c (MPa):

$$\sin \phi = b \cdot (\sigma_1 + \sigma_3)^d$$

where

$$b = 1.30 - 0.017\,\gamma - 0.028\,\Delta D$$

$$d = -0.234 - 0.001\gamma - 0.0007 \cdot \Delta D + 0.048\,\rho$$

and

$$c = -3.2 + 0.144\,\gamma + 0.071 \cdot \Delta D + 1.5\rho$$

The correlation coefficient 0.998 is slightly higher than the correlation coefficient from the previous analysis and the standard deviation is smaller (0.68 compared to 0.88 MPa).

Although the result is not significantly better, the difference is obviously explained by the abovementioned fact.

Creep Behaviour

As mentioned previously, the number of applicable creep tests in the data base is very limited, which certainly is reflected in the result of the regression analysis.

It has only been possible to estimate a few empirical constants and the results do not match general experience very well.

For the Menzel-Schreiner type of creep law the following results are found

$$A = 0.035+0.0028\cdot(a/c^*)-0.039\ EFF$$

$$m = 1.0$$

$$n = 1.01$$

with correlation coefficient r = 0.93 and standard deviation 0.073 on the creep strain.

Alternatively using the logs we find a somewhat better result

$$A = 0.026 + 0.42\cdot10^{-4}\gamma + 0.19\cdot10^{-3}\cdot\Delta D - 0.012\rho$$

$$M = 0.58+0.14\cdot10^{-2}\gamma + 0.012\cdot\Delta D$$

$$n = 2.18+0.016\gamma + 0.57\cdot10^{-3}\cdot\Delta D$$

with r = 0.98 and standard deviation equal to 0.039 on the creep strain.

The last results seem reasonable, but still not acceptable for design purpose due to insufficient data.

8. DISCUSSION OF RESULTS

The analytical work conducted on the basis of the available Tostrup salt data demonstrates the possibilities of correlation analysis as well as general regression analysis.

Due to various limitation in the quantity and quality of the data available, the specific results produced for engineering purposes do not cover all aspects of salt behaviour.

Concerning salt strength, the general regression analysis produces results applicable for design purposes, but only

for the Tostrup salt dome and only the Zechstein 2 salt in this dome from which nearly all data are collected.

Contrary to the normal data evaluation as it appears in f.ex. the design documents for the Tostrup salt caverns, the analysis applied in this project introduces some new aspects in the use of various types of data from the salt dome.

It clearly appears from the previous section that the strenght properties of the salt can be correlated in a quantitative way to other salt data, which means that the huge amount of f.ex. log data can be used in a much more direct way than previously in the definition of the rock mechanical basis for design analysis of cavern behaviour.

9. FURTHER RESEARCH

In our opinion this project has demonstrated very interesting possibilities in systematic statistical analysis of salt properties.

In order to increase the confidence in the results of such analysis it is of great importance, that the amount of data describing fabric and texture of the salt samples is increased and that more time is spend in detailed evaluation and analysis of creep tests. It appears that the simple digitizing of creep curves (as applied in this context) is insufficient and inaccurate. Future work should be based on more refined handling of test raw data.

Provided these steps are taken, it is very likely that structural data may replace the more expensive mechanical tests to a certain extent and that logs can be used for more reliable extrapolation between the cores taken in a well.

10. REFERENCES

/1/ EFP-81

/2/ Naturgaskoordinationsudvalget (NKU), 1982: Guidelines for the Design of Underground Caverns in Salt for Natural Gas Storage.

/3/ D.O.N.G. A/S, (1979-83): projekt material for the L1.Torup storage project prepared by

NGG, Naturgasgruppen
RISØ, forsøgsanlæg
LUB, Lehrgebiet, Unterirdicher Bauen, Universität Hannover
ABK, Afdelingen for Bærenden Konstruktioner, DTH
KBB, Kavernen Bau und Betriebs-GMBH, Hannover.

/4/ Larsen, J,G., in press: "New methods in Textural and Fabric Analysis of Rock Salt Related to Mechanical Test Data, Tostrup Salt dome, Denmark. Sixth International Symposium on Salt.

/5/ Ottosen, N.S. and Krenk, S., 1980: "Material Models for Rock Salt and Calculations for Gas and Oil Storage Cavities", RISØ-M-2277.

/6/ Lagoni, P., 1976: "Mechanics of granular Materials", Ph.D. thesis, The technical University of Denmark.

S A L T R E S E A R C H P R O J E C T E F P - 8 1

Volume I. Sammendrag af Saltforskningsprojekt EFP-81. (English summary).
Editor: J.Fabricius.

Forord.

Historisk oversigt.

Kapitel 1. Stratigrafi.

Kapitel 2. Stensaltets texturelle opbygning.

Kapitel 3. Mikrotermometri.

Volume II. Stratigraphy.

Chapter 1. Lithostratigraphy of the Zechstein Salts in the Norwegian-Danish Basin.
Fritz Lyngsie Jacobsen.

Chapter 2. Description of the Dolomite-Anhydrite Transition Zone (Zechstein 1 - Zechstein 2) in the Batum-13 well, Northern Jutland, Denmark.
Martin Sønderholm.

Chapter 3. A geochemical study on Zechstein Salt and Anhydrite from the Batum-1A well.
Niels Springer.

Volume III. Fabric Analyses of Domal Rock Salt.

Chapter 1. Textural and Petrofabric Analyses of Rock Salt related to Mechanical Test Data - a quantitative Approach.
Jørgen Gutzon Larsen.

Chapter 2. Statistical Analyses of Mechanical Properties of Rock Salt.
Per Lagoni.

Volume IV. Microthermometry.

Chapter 1. Studies of Fluid Inclusions in Halite and euhedral Quartz Crystals from Salt Domes in the Norwegian-Danish Basin.
Johannes Fabricius.

Chapter 2. Formation Temperature and Chemistry of Brine Inclusions in euhedral Quartz Crystals from Permian Salt in the Danish Trough.
Johannes Fabricius.

Chapter 3. The Thermal Stability of Natural Carnallite in Cognate Geological Environments.
Johannes Fabricius.

Fabric studies have been performed on rock salt cores from salt domes as part of a general structural study with the purpose of quantifying textural descriptions and relating them to uniaxial compression strength of the rock salt.
New methods of preparation of test samples are introduced: acetate replicas of cut core samples and turned spheres of the cores, overgrown with cubelets of NaCl.
The replicas are used in connection with automatic image analyser in order to determine the elliptic form factor, the specific grain perimeter and the areas and the long axes of flattened grains and the periphrastic ellipsis. The spheres are mounted at an oversize universal stage and the orientation of the crystallographic axes are established.
The characteristic mechanical salt parameters have been collected and treated statistically. A correlation analysis and a regression analysis have been carried out. The salt strength has been correlated with the salt structure and log results. The creep behaviour of the rock salt tested is discussed.

Geological Survey of Denmark
Thoravej 31
DK 2400 Copenhagen
Denmark
Phone + 45 1 10 66 00

ISBN 87 88640 08 6 (bd.1-4)